A CHIRP z-TRANSFORM ALGORITHM FOR PROCESSING DOPPLER ULTRASOUND FLOWMETRY SIGNALS

BY

ANNE KATHRYN DELK

B.S., University of Illinois, 1980

THESIS

Submitted in partial fulfillment of the requirements
for the degree of Master of Science in Electrical Engineering
in the Graduate College of the
University of Illinois at Urbana-Champaign, 1982

Urbana, Illinois

ACKNOWLEDGEMENTS

I would like to express my appreciation to my advisor, Dr. W. D. O'Brien for his suggestion of this thesis topic and his advice throughout the work.

In addition, I would like to thank Steve Foster for his constant, invaluable assistance with the data acquisition system and the programs, and Bill McNeil for his work in building the flow system.

Special thanks are extended to my parents and brothers for their encouragement and support during my education, and to Ken Fullett for his advice, encouragement, patience, and understanding throughout this thesis.

TABLE OF CONTENTS

CHAPTER 1

INTRODUCTION

The knowledge of cardiac parameters such as cardiac output and blood flow or blood velocity profiles are important for cardiovascular diagnostic purposes and physiological studies. The study of cardiovascular parameters has become increasingly important with the large growth in cardiovascular disease, especially coronary artery disease. A blood flow profile is the output volume rate of blood as a function of position in the vessel. A blood velocity profile is the rate the blood is moving as a function of position in the vessel. Stenosis or occlusion of blood vessels can be detected by examining the vessel flow pattern for local flow disturbances such as increased blood velocity or flow turbulence in a small section of the vessel. Besides the coronary arteries, the detection of stenosis is important for all parts of the vascular system. In addition to assisting in assessing vascular disease, blood flow and blood velocity waveforms provide a clearer picture of the vascular system.

Many flow and velocity measurement techniques are available. Blood flow can be obtained from blood velocity by multiplying the blood velocity by the cross sectional area of the blood vessel. Often, blood flow and blood velocity are interchanged, but it must be remembered that the cross sectional area of blood vessels is not constant. There are two important properties of a blood velocity measurement technique. The first important and obvious property of a blood velocity measurement technique is the output should be proportional to the velocity of the blood. Therefore, it should be independent of, or take into account, the blood vessel size, vessel wall

properties, and blood hemocrit. The second important property of a blood velocity measurement technique is it should not disturb or disrupt the flow; specifically the technique should be non-invasive.

1.1 Ultrasonic Flowmetry

There are many velocity measuring techniques available. Most of these techniques are invasive. Ultrasonic flowmetry is a non-invasive velocity measurement technique. Ultrasound is high frequency sound (pressure) waves above the audible frequency of 20 kHz. To measure blood velocity a beam of ultrasound is passed through the blood vessel, and blood velocity information in the vessel is detected by one of two methods. The two velocity measurement methods used in ultrasonic flow velocimeters (ultrasonic flowmeters) are the transit time technique and a technique based on the Doppler principle.

The transit time technique measures fluid velocity by the time difference for ultrasound to propagate in one direction compared to another direction along the same path (Bergel, 1972). The average fluid velocity is determined by the difference between upstream and downstream transit times, provided the velocity of sound in the fluid and the angle between the sound beam and the flow axis is known. Alternatively, the average fluid velocity is determined by measuring the difference in phase shifts between transmit and receive signals, and taking the difference between the upstream phase shift and the downstream phase shift. The upstream and downstream signals can be sent alternately, or if two different frequencies are used, the upstream and downstream signals can be transmitted simultaneously.

The second velocity measurement technique used in ultrasonic flowmeters measures the fluid velocity by the Doppler effect. The velocity is determined by the frequency shift of sound which is backscattered from moving particles in the fluid, the red blood cells. There are several methods used to measure this Doppler shift. The ultrasonic beam can be continuous wave or pulsed. In both cases two transducers, one to transmit and one to receive, can be placed on opposite sides of the vessel or both transducers can be placed on the same side of the vessel. In the case of pulsed ultrasound, one transducer can be used for both transmit and receive.

1.2 The Doppler Effect in Blood

Doppler ultrasonic flowmetry depends on the interaction of ultrasound with moving blood. Blood is a viscous fluid composed principally of red blood cells, white blood cells, and platelets suspended in plasma. The primary source of ultrasonic scatterers in blood is the red blood cells (Shung et al., 1976). The number of red blood cells is over 500 times the number of white blood cells and the volume of a red blood cell, 45.0 ml/100 ml of blood, is much greater than the volume of a platelet, 0.3 ml/100 ml of blood (Wintrobe, 1967). In normal blood, the scattering from white blood cells and platelets is negligible.

Red blood cells are biconcave disks. The average diameter of a red blood cell is 7 μm, and the average thickness is 2 μm. Red blood cells are very small compared to the wavelengths of ultrasound. The density of red blood cells is 1.092 g/cm^3 and of plasma is 1.021 g/cm^3. The adiabatic compressibility of red blood cells is 34.1×10^{-12} cm^2/dyne, less than that

of plasma which is 40.9×10^{-12} cm^2/dyne. The density of the scatterers, the red blood cells, is greater than that of the fluid, plasma, and the adiabatic compressibility of the scatterers is less than that of the fluid. Because of its small size and its acoustic characteristics, the backward scattering of red blood cells is larger than the forward scattering, and the scattering cross section can be calculated. The scattering cross section also depends on the ultrasonic frequency and blood hemocrit. For normal blood, at an ultrasonic frequency of 5 MHz, the volumetric scattering cross section is 4.5×10^{-14} cm^2 (Shung et al., 1976). Because the scattering cross section is so small, the red blood cells reflect almost all of the ultrasonic energy transmitted into the vessel.

Consider a Doppler velocity measurement of a single red blood cell as shown in Figure 1.1. One transducer is used for both transmitting and receiving the ultrasonic signal. The single red blood cell is moving at a constant velocity, v, away from the transducer in the blood vessel. The total transmission path of the ultrasonic signal, x, is measured from the transducer to the red blood cell and back to the transducer. The path will be linearly increasing with time as the red blood cell travels, causing a linearly increasing phase shift between the transmitted and received signal.

If the transmitted signal is $\cos 2\pi Ft$, and the sound beam is along the flow axis, the normalized received signal, r(t), will be:

$$r(t) = R \cos 2\pi F[t + (2\Delta x/c)] , \qquad (1\text{-}1)$$

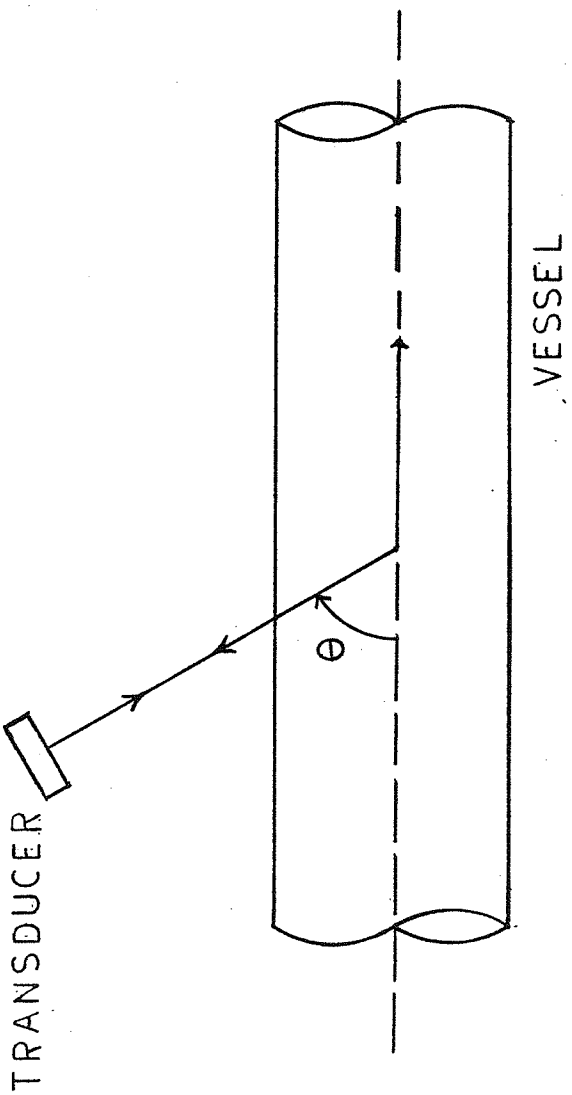

Figure 1.1. The geometry of a Doppler flow measurement from a single red blood cell.

where Δx is the additional path length of the ultrasonic signal due to the moving red blood cells, c is the propagation velocity of sound, and R is the magnitude of the reflected power. If the path, Δx, is linearly increasing at a rate corresponding to the velocity of the red blood cell, v, then the received signal is:

$$r(t) = R \cos 2\pi F[t + (2v/c)t] \ . \qquad (1\text{-}2)$$

There is a phase difference between the transmitted and received signal of $2Fv/c$. Frequency is defined as the rate of change of phase. Therefore, there is a change in frequency which is proportional to the velocity of the red blood cell: $\Delta f = 2Fv/c$. This change in frequency is called the Doppler shift. If the transducer subtends an angle with the flow axis, the magnitude of the Doppler shift corresponds to the velocity component along the sound beam axis. The Doppler shift detected from a moving red blood cell at an angle θ, with respect to the sound beam axis is defined:

$$\Delta f = 2Fv(\cos \theta)/t \ . \qquad (1\text{-}3)$$

1.3 Doppler Ultrasound

The early Doppler ultrasonic flowmeters for measuring blood velocity were continuous wave ultrasound systems. These continuous wave Doppler ultrasound systems used two transducers placed on opposite sides of the blood vessel. One transducer continuously transmitted a single frequency ultrasound beam into the vessel and the other transducer received the signal scattered by the red blood cells. The scattered signal was mixed with the transmitted sound and the frequency shift was measured by either

a simple zero crossing frequency meter or by taking the derivative of the signal with a simple analog amplifier. The latter method is difficult to implement because the output is dependent on the amplitude, as well as the frequency, of the scattered signal.

These initial Doppler ultrasonic blood flowmetry systems were non-directional; they were unable to determine the flow direction. McLeod solved this problem by quadrature phase detection (Baker et al., 1978). The directional velocity signals are obtained by the single sideband receiver technique, which separates the upper and lower sidebands by using a pair of phase detectors.

Pulsed Doppler ultrasound systems were developed to solve the range limitations of continuous wave Doppler ultrasound systems. Continuous wave Doppler flowmeters detect all motion in the sound path. Therefore, they have no range, or spatial, resolution. Variation of velocity in the vessel cannot be detected. Pulsed Doppler systems use range gating so that each ultrasound pulse corresponds to a particular depth.

One step beyond the pulsed Doppler system is the Duplex system. The Duplex system, a combination of two-dimensional imaging with pulsed Doppler flow detection (Barber et al., 1974), was developed to provide more information about the vessel diameter and orientation of the Doppler sound beam with respect to the flow axis. The previous systems cannot accurately determine velocity without additional information about the angle between the sound beam and flow axis.

Recent improvements to the Duplex systems have been in transducer design and in faster, more accurate processing of the returned signal. With the advances in digital signal processing, more techniques are

available to process these Doppler ultrasonic blood flowmetry signals. The purpose of this thesis is to investigate the possibility of using digital signal processing techniques developed for radar applications to process Doppler ultrasonic blood flowmetry signals. By transforming the Doppler signal into the frequency domain, the Doppler shift can be quantitatively determined.

This velocity measurement technique will consist of irradiating the vessel with a pulse of ultrasound. The return echo backscattered from the red blood cells versus time will be digitized. First, the digitized signal will be processed by dividing the signal into small blocks, with each block corresponding to a particular depth into the vessel. Each block will be multiplied by a window, or weighting function, to enhance the spectral resolution. Then, each block will be transformed into the frequency domain by the chirp z-transform technique. The frequency at each depth will be compared to the transmitted frequency to determine the Doppler frequency shift, which can be used to calculate the velocity.

CHAPTER 2

BLOOD FLOW MODEL

A mathematical model for blood flow is necessary to fundamentally investigate any technique for extracting Doppler ultrasound blood flow signals. To this end, a brief discussion of hemodynamics, the study of blood flow, is provided, and details the blood flow model. The model must be one in which there is a well characterized solution for the fluid velocity so that the results of this velocity measurement technique can be compared to theoretical values of velocity.

2.1 Hemodynamics

Researchers have investigated blood flow in the attempt to characterize the circulatory system, including blood velocity profiles of the vessels. The modeling of the circulatory system, including blood flow and velocity, has been studied for many years, since William Harvey's classical description of the circulation of the blood (Noordergraf, 1969). In the eighteenth century, Euler began to relate velocity to pressure gradients, and by the twentieth century two different theories of blood flow had developed.

One theory of blood flow is the windkessel theory (Noordergraf, 1969), which has been greatly criticized and generally unaccepted, although it has not been entirely abandoned (Noodergraf, 1978). The windkessel approach to the modeling of the circulatory system is based on the premise that arteries behave as reservoirs, capable of storing blood (Noordergraf, 1969). Blood is pumped in at one end intermittently, while the outflow is constant.

The storage capacity is determined by the modulus volume of elasticity, E': $E' = dp/dV$, where V is volume. The pressure and flow of a section of blood vessel are related by equating the difference between inflow and outflow of the section of blood vessel, to its rate of storage. All pressure changes are considered to occur simultaneously, which implies the blood travels at an infinite wave velocity (Noordergraf, 1978).

The pulse-wave velocity theory is generally accepted as the better approach to the modeling of the arterial system (Noordergraf, 1969). The approach, largely developed by Witzig in 1914, consists of three parts, viz., the equations of motion of the blood, the equations of motion of the blood vessel, and the boundary conditions (Cox, 1969). Blood is assumed to be an incompressible, Newtonian viscous fluid. Also, axisymmetric laminar motion is assumed. The equations of motion of the fluid are described by a linearized axisymmetric set of Navier-Stokes equations, one for the longitudinal fluid velocity and one for the radial fluid velocity. The two fluid velocities are related by the equation of continuity. The boundary conditions consist of the continuity of velocity at the center of the vessel and at the vessel walls, and the continuity of stress at the inner and outer walls of the vessel.

Most research and discussion of the pulse-wave velocity theory is devoted to the equations of motion of the vessel. The major source of disagreement is in the modeling of the vessel wall. Two different equations of vessel motion have been developed. There is an equation of motion based on a thin-walled, elastic membrane vessel wall and an equation of motion based on a thick-walled elastic vessel. In addition, there are two models of vessel wall viscoelasticity (Cox, 1969). Each of these two

models of viscoelasticity produces an expression to replace the Lamé constants. The expression is substituted into the thick-walled elastic vessel equations of motion. The Voigt model pictures the vessel wall mechanically as a spring in parallel with a dashpot. It is more commonly used than the standard linear solid model developed by Cox which pictures the vessel wall mechanically as a spring in series with the spring and dashpot parallel combination. Of the four different views of the vessel equations of motion, the Voigt model of viscoelasticity replacing the Lamé constants in the thick-walled approach is used the most, but none of the models has been fully investigated.

With the advent of computers, for any one of these assumptions, pressure and flow at each point in space and time can be calculated individually, knowing the pressure or flow at the previous point. The equations of the blood flow system are transformed into finite difference equations form. For example, the two differential equations of the pulse-wave velocity approach are replaced by two finite difference equations. The boundary conditions and the parameters of the system can be changed and new velocity profiles can be plotted (Kufahl, 1980). The effects of each parameter can readily be seen.

Although many researchers have investigated various properties of blood vessels, there is not much information available on the values of the needed physical parameters. Blood vessels are cylindrical tubes which vary in diameter up to 3 cm. The elasticity and thickness of the vessel walls vary greatly with age, health, and location in the cardiovascular system. The thickness of the vessel walls is usually 2 mm or less. An approximate value of Young's modulus of arteries is on the order of 10^6 g/cm s^2.

2.2 The Flow Model

Because of the many blood flow models available, and because the calculations of blood flow are very complex in most cases, a simple experimental model was chosen to test the ultrasonic blood velocity measurement technique. Blood flowing in a vessel was modeled by simple flow of a viscous fluid containing ultrasonic reflectors through a thin-walled rigid tube. The velocity profiles were predicted and thus, the experimental profiles were comparable to the theoretical profiles.

2.2.1 Simple Flow

The simplest model of fluid flow is steady, uniform, laminar flow through a pipe. Steady flow means the velocity of the fluid is independent of time and only a function of position. In reality, steady flow is rarely encountered, but steady flow can be approximated when the flow varies about the mean flow (Pao, 1961). Uniform flow occurs when the velocity is independent of distance along any streamline. Therefore, the flow is straight and the streamlines are all parallel to themselves and the boundaries (Roberson and Crowe, 1975). Laminar flow is nonturbulent flow; specifically the velocity is low enough so that the flow is straight and parallel to the boundaries and the fluid appears to move in layers sliding over each other (Pao, 1961). Finally, the pipe is a fixed, rigid closed conduit.

The velocity profile of steady, uniform, laminar flow through a cylindrical pipe, taking into account the viscosity of the fluid, is given by

$$u = (1/4\mu)\ (dp/dx)\ (R^2 - r^2) \qquad (2\text{-}1)$$

where u is the radial velocity of the fluid, μ is the shear viscosity of the fluid, p is the pressure, x is the distance along the pipe, r is the radial distance, and R is the radius of the pipe. The result is a parabolic velocity profile. The corresponding volume rate of flow is given by:

$$Q = (\pi R^4)/(8\mu) \ (dp/dx) \qquad (2\text{-}2)$$

where Q is the volume rate of flow (Sharpe, 1967).

2.2.2 The Flow System

The model flow system used in the experimental portion of the project is pictured in Figure 2.1. A variable speed pump, controlled by a Variac, is connected to the reservoir of fluid. The output port of the pump is connected to the tank. The tank is constructed of Plexiglas and a 1.59 cm inner diameter, 1.61 cm outer diameter, thin plastic tube was inserted crosswise through the tank. The other side of the tank is connected to the reservoir of fluid, completing the flow circulation. The tubing connecting the reservoir to the pump and that connecting the pump to the tank is 1.90 cm inner diameter tubing, and 1.59 cm inner diameter tubing connects the tank to the reservoir. The same size or smaller diameter tubing as compared to the plastic tube was necessary in connecting the tank to the reservoir to avoid converging flow, which created turbulence and caused some difficulty in calculating the actual fluid flow and fluid velocity in the tube.

The fluid used in these experiments was whole milk. Milk has been used by other researchers to simulate blood in flow experiments (Flax, et al., 1971; Choi, 1978). Milk is viscous and contains fat, protein, and

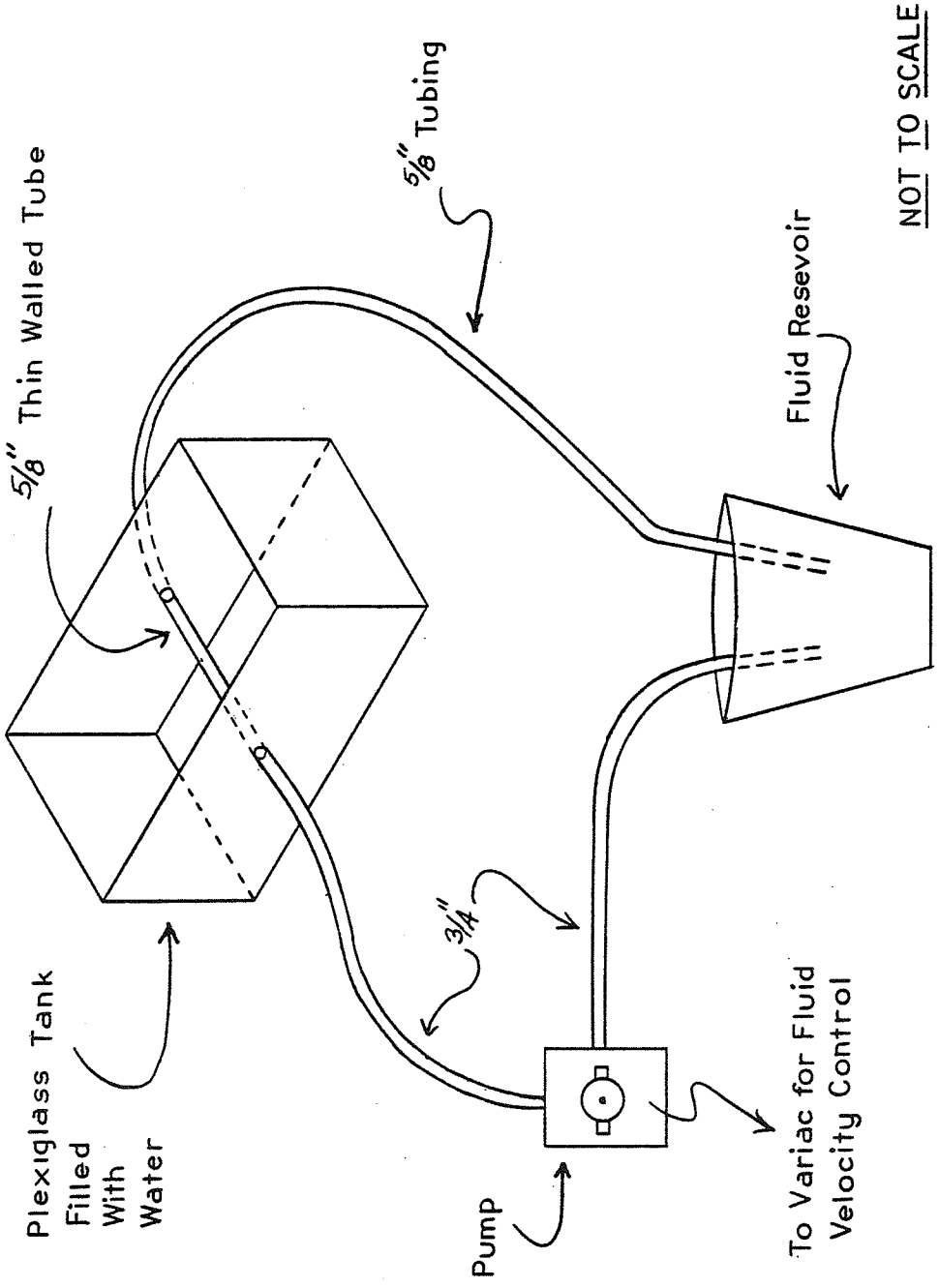

Figure 2.1. The experimental flow system.

lactose particles which are ultrasonic scatterers. The speed of sound in milk is 1540 m/s, at 20° C (Goss et al., 1978). The viscosity of milk and blood are approximately the same. The relative viscosity of healthy human blood is 3.5-5.4, at 20° C. Therefore, the viscosity of blood was used in the calculations to estimate the fluid velocity.

Flow measurements were made as follows in order to estimate the fluid velocity and corresponding Doppler frequency shift. The pump was started and the fluid set to a constant velocity. After the initial turbulence had subsided, the fluid velocity was calculated by measuring the time the fluid took to fill a 400 ml beaker. From the volume rate of flow equation (2-2) the pressure gradient can be calculated, which is needed to calculate the fluid velocity, equation (2-1). At the medium speed setting, the maximum fluid velocity was calculated to be approximately 2 m/s at the center of the tube, which is the expected maximum velocity of blood in healthy humans. Using equation (1-3), the Doppler frequency shift was calculated, assuming a transmitted frequency of 5 MHz. At an angle of 45 degrees, the Doppler frequency shift is 9 kHz. At the high speed setting, and at an angle of 45 degrees, the maximum expected Doppler frequency shift is approximately 15 kHz.

CHAPTER 3

THE EXPERIMENT

The experimental procedure consisted of several steps. The first step was to develop and construct the model flow system as described in Section 2.2.2. Next, the A-scan acquisition system was reconfigured from existing equipment and interfaced to a digitization system. The analog A-scan signal (return ultrasound echo versus time) was viewed on an oscilloscope for optimization of the electronic and flow system parameters. The data, sets of digitized A-scan signals, were stored in a computer to be later processed by the windowing and chirp z-transforming technique described in Section 1.3. The output from this signal processing technique was frequency versus depth, or axial position along the A-scan beam. Then, this frequency data could be transformed into the velocity profile by multiplication of a constant.

3.1 The Measurement and Digitization System

The flow system consisted of a Plexiglas assembly tank filled with water in which a plastic tube through which the scattering material flowed and was connected to an external flow control. Water, rather than air, was used as a coupling medium to provide a closer impedance match to the plastic tube. The characteristic impedance of plastic is approximately 3×10^6 rayls. The characteristic impedance of water is 1.48×10^6 rayls, while that of air is only 415 rayls. Using air as a coupling medium the power transmission coefficient is less than 1%, and using water the power transmission coefficient is greater than 95%, assuming normal incidence and

a thin-walled plastic tube. With water as a coupling medium, more sound will be transmitted into the tube and more sound reflected by the scatterers will be transmitted out of the tube. The tank of water was allowed to set for several hours or longer before taking data, to eliminate air bubbles which would scatter the sound.

The velocity of the fluid was detected by the shift in frequency of ultrasound as discussed in Section 1.2. The tube was irradiated by a pulse of ultrasound transmitted from a Panametrics 5 MHz center frequency, broadband transducer. The ultrasound reflected by the fat, protein, and lactose particles in the milk is received by the same transducer. The transducer was placed in the tank of water at approximately 45 degrees to tube, and several centimeters away (Figure 3.1). Ideally, for Doppler information, the transducer should be parallel to the flow, and for imaging information, the transducer should be perpendicular to the tube. Imaging information was necessary to determine where the walls of the tube were located and therefore, where the Doppler information was located. Furthermore, it is not physically possible to noninvasively place the transducer parallel to the flow in this situation or in the situation of actual blood velocity measurements.

A block diagram of the measurement and digitization system is shown in Figure 3.2. The 5 MHz Panametrics transducer is controlled by a Panametrics pulser/receiver, model 5050 PR. The pulser/receiver generates a large amplitude, short pulse and sends it to the transducer, which produces a burst of ultrasound. The pulser/receiver has variable settings for energy and damping factor. For all experiments, the energy control was set to the maximum, a setting of 4. This selects a maximum electrical

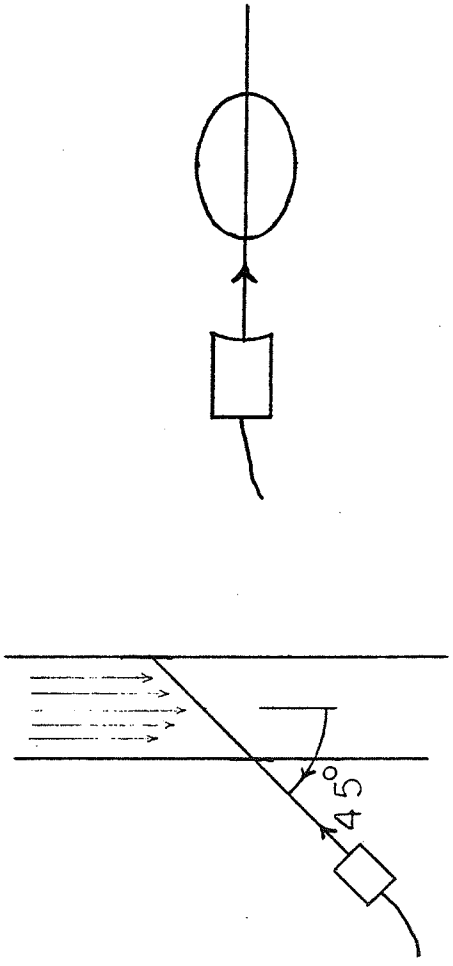

Figure 3.1. Orientation of the measurement tranducer to the vessel.

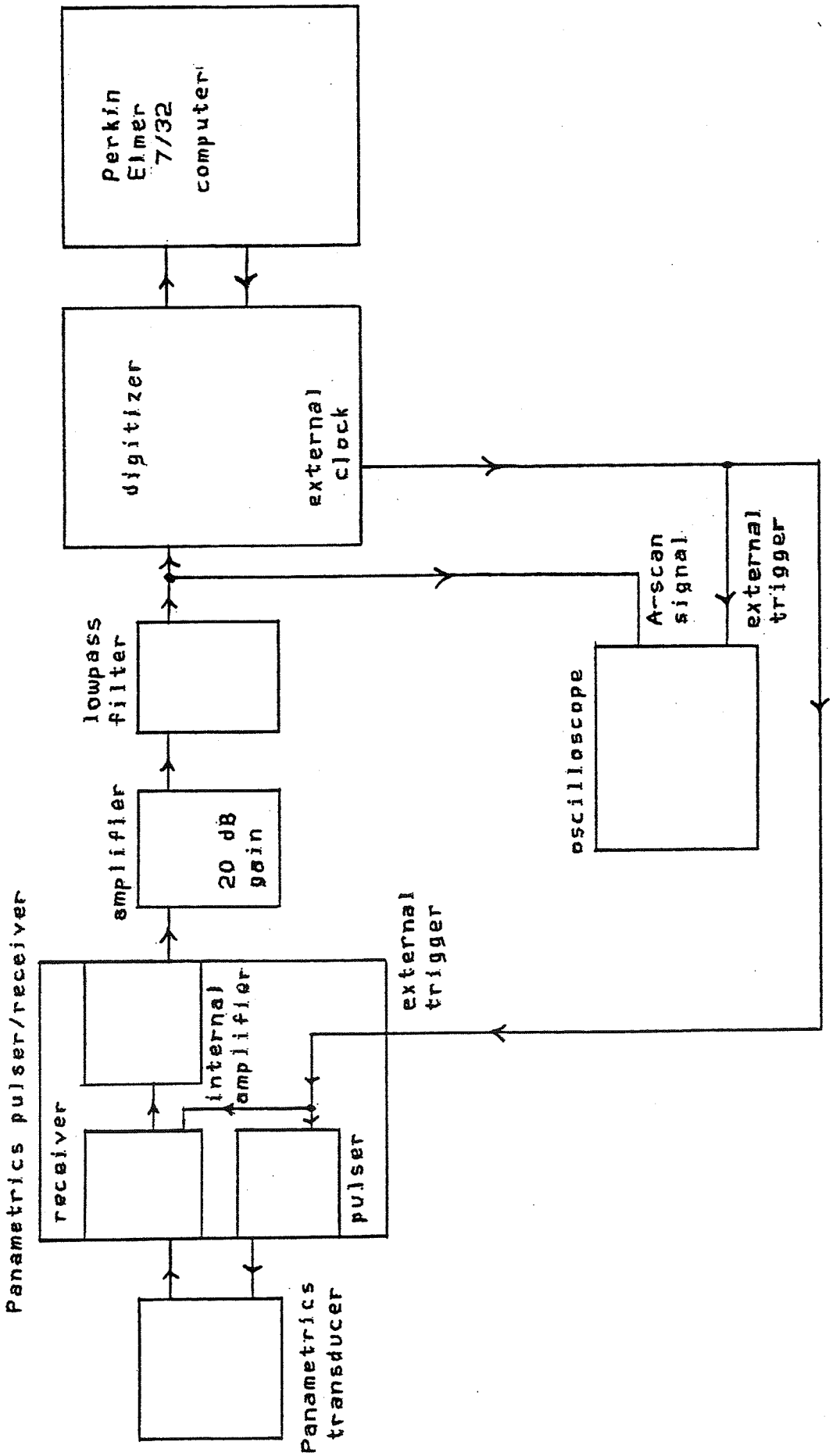

Figure 3.2. Block diagram of the measurement and digitization system.

pulse amplitude of about 250 volts. The damping factor varies the resistive load to the transducer. Higher damping, or lower Q factor, produces better range resolution. The damping factor control was set to 6, selecting a resistive load of approximately 150 ohms.

After the pulser/receiver sends the pulse, it switches to accept the return A-scan signal received by the transducer. The pulser/receiver was triggered externally by the digitization unit. The received A-scan signal is sent to an amplifier. The amplifier provides a voltage gain of 100. Then the amplifier is followed by a variable attenuator. The variable attenuator was set at 0 dB for all experiments. These settings produced optimal A-scan signals as viewed on the oscilloscope.

The ultrasonic energy reflected from the milk is very small, less than half the amplitude of the reflected signal from the tube walls. Since even the reflected signal from the tube walls was too small to digitize with maximum energy and 0 dB attenuation settings, an amplifier was inserted after the pulser/receiver. The Hewlett-Packard 461A amplifier provided 20 dB gain. A 3 pole Butterworth matched filter, with a cutoff frequency of 8 MHz, followed to eliminate high frequency noise.

The A-scan signal was digitized by an analog-to-digital (A/D) converter unit controlled by the Perkin-Elmer Model 7/32 (Foster, 1981), hereafter referred to as the 7/32. The data acquisition system, originally designed to digitize video images, consists of an r-f amplifier, a digitizer, and the 7/32. The digitizer controlled by the 7/32 was used to digitize the A-scan signal. The digitizer consists of a 30 MHz A/D and a high speed buffer memory.

The A/D was modified to operate an effective rate of 88.45 MHz, providing the signal under investigation is assumed to be periodic. Instead of triggering off the beginning of every sync signal, the A/D was triggered off consecutive quarter cycles of the sync signal. The first point of the A-scan signal is digitized when the A/D is triggered by the beginning of the sync signal. The next point of the A-scan signal is digitized when the A/D is triggered, not by the beginning of the next cycle, but by the next fourth of the cycle. Each time the A/D is triggered a fourth cycle later. Therefore, the effective digitizing frequency was increased fourfold from the actual rate the A/D was operating, viz., 22.118 MHz. A block diagram of the modified digitization system is shown in Figure 3.3.

This method of increasing the sampling frequency is valid if the signal is periodic. Although the A-scan signal was not long-term periodic, it was short-term periodic. Within the time necessary to digitize a single A-scan, the signal was periodic. Within the time necessary to capture several signals and average them, the small fluctuations in the fluid flow effected the digitized output so that each successive signal was different than the previous one, and averaging several signals degraded the digitized output. Therefore, this digitization method is valid for single Doppler signal extraction.

To digitize a signal, the following information had to be provided: the delay from the beginning of the trigger signal, the number of data points desired, the number of times the signal is to be averaged, and the file in which to store the data. The delay can be estimated by examining the A-scan signal on the oscilloscope. The oscilloscope is triggered by

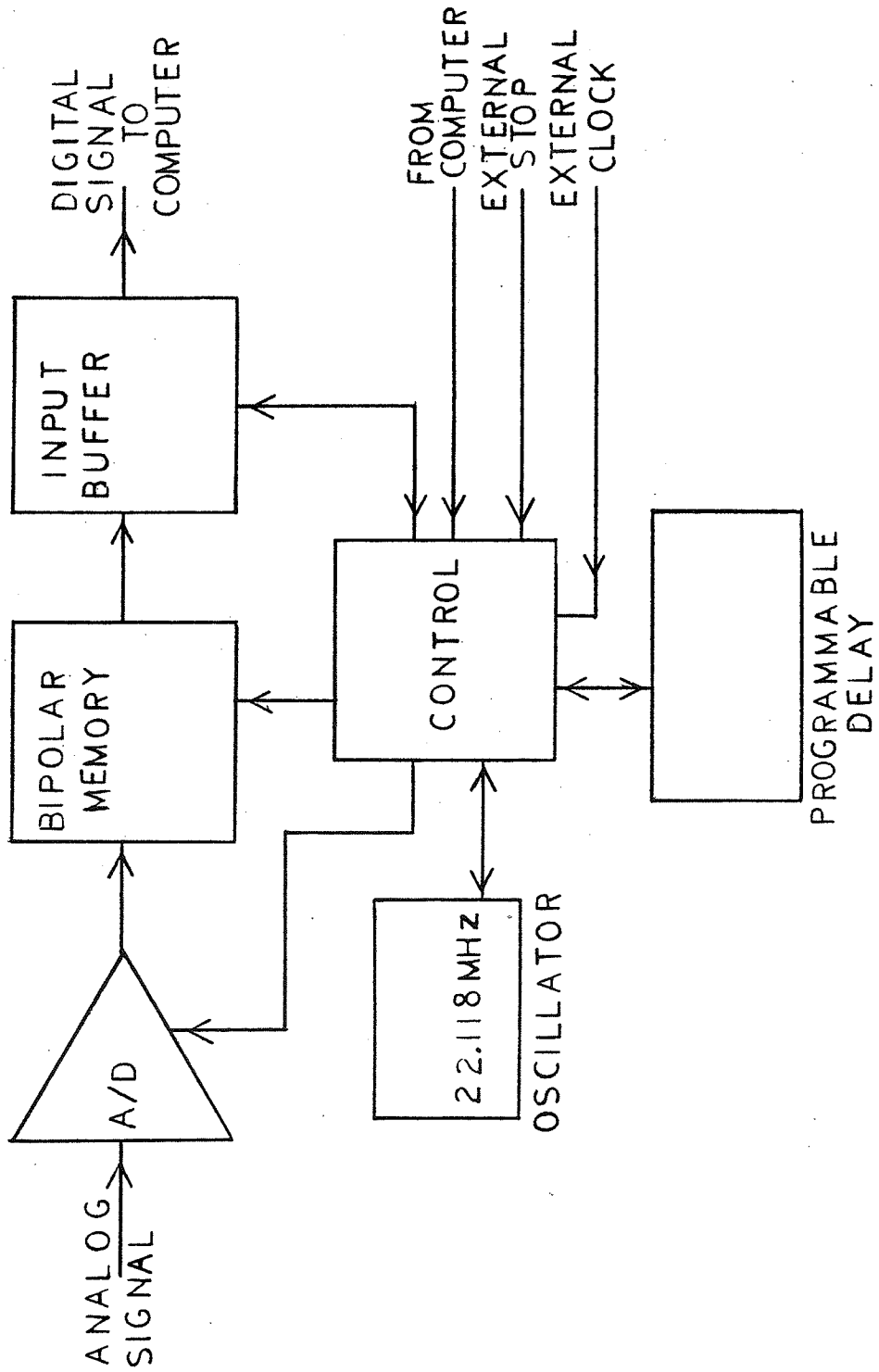

Figure 3.3. Block diagram of the modified digitizer.

the same trigger signal sent from the digitization unit to the pulser/receiver. The delay is the number of seconds from the beginning of the A-scan signal to the first large perturbation, which in this case is the reflection off the first wall, multiplied by the oscillator frequency of 22.118 MHz. From the plotted digitized A-scan signal, the delay could be fine tuned. Usually the first 2048 points of the digitized A-scan signal were stored. The signal was only averaged once. Although averaging improves the signal-to-noise ratio, as previously stated, the digitization method is not valid for multiple averages of this A-scan signal. A sample digitized A-scan signal is shown in Figure 3.4.

3.2 Processing

Each A-scan signal was processed by moving a window across the signal and performing a chirp z-transform on each windowed group of points. Moving a window across the data separates it into a set of signals, each one corresponding to a particular depth or axial distance from the transducer. The chirp z-transform algorithm was performed on each windowed data set, transforming each one from the time domain into the frequency domain. The frequency which contained the maximum energy of the spectrum for each depth is plotted, and with a change of scale by multiplication of a constant, forms the velocity profile. The windowing technique, the chirp z-transform algorithm, and the program are discussed in the following subsections.

3.2.1 Windows

Physical constraints require that digital signal processing techniques utilize data which are finite in length or time limited. Time limiting

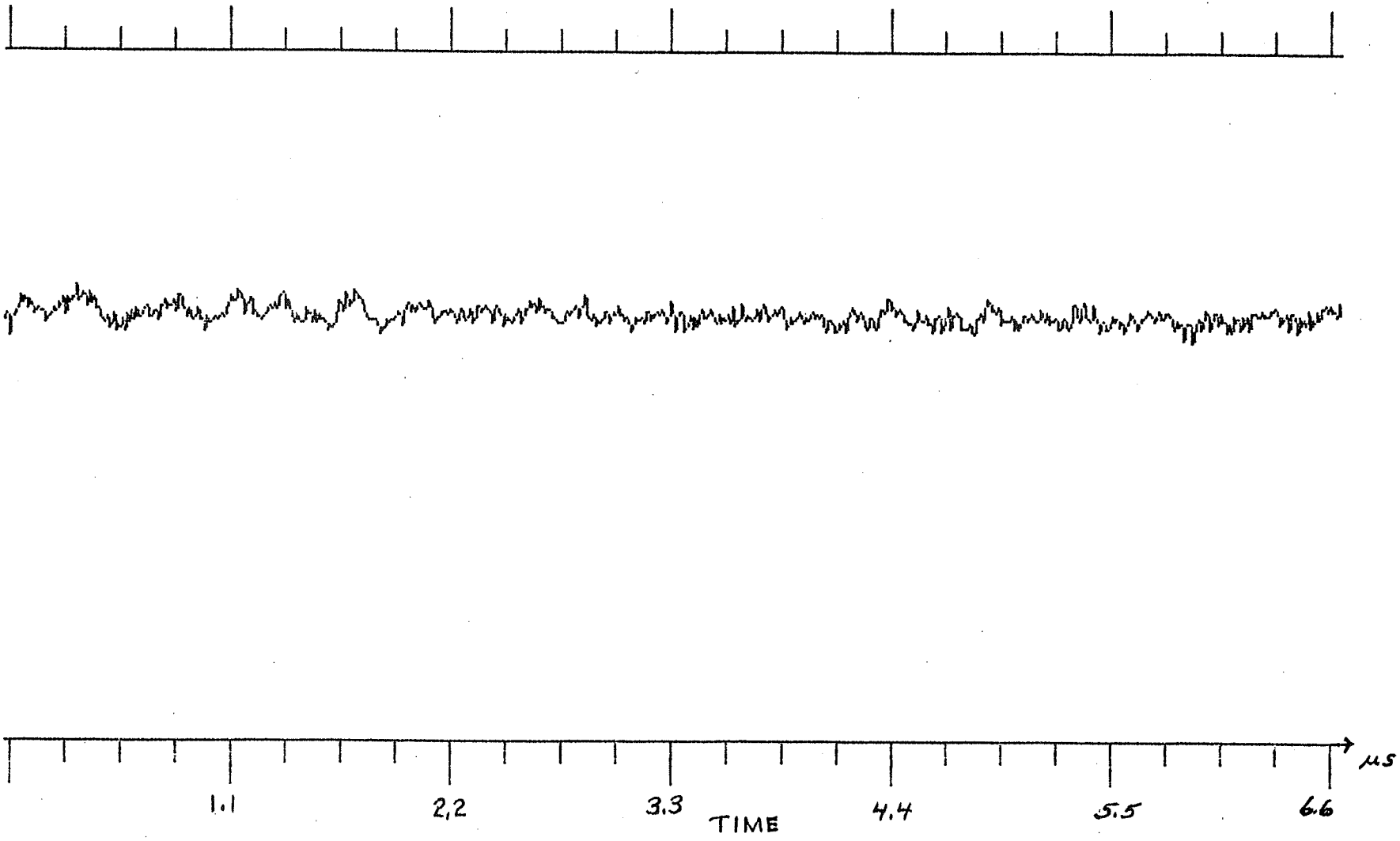

Figure 3.4. A sample digitized A-scan signal.

any sequence results in the convolution of the Fourier transforms of the sequence with the Fourier transforms of the truncating function (Childers and Durling, 1975). This causes the estimate of the frequency spectrum to spread out and to smear or leak into adjacent frequencies and side lobes. The effect is called spectral leakage. At the same time, there is a loss of resolution between adjacent frequencies since energy from each frequency smears into the spectrum of the surrounding frequencies. A single frequency component will appear as a spectrum of several frequencies and the spectrum of two adjacent frequencies will overlap.

To minimize this difficulty, weighting functions, or windows, are multiplied to sequences, to not only truncate the sequence, but to reduce the spectral leakage due to truncation (Harris, 1978). The Fourier transform of a window is a large main lobe centered about zero, and smaller side lobes decreasing in amplitude at each side, continuing infinitely in frequency. Since the Fourier transform of a window extends infinitely in frequency, the convolution of it with the Fourier transform of the sequence is not bandlimited. Therefore, a finite spectrum becomes infinite in the estimation.

In a sense a window is a filter, collecting contributions over its frequency extent for the spectral estimate. Just as the bandwidth of a filter is important, the bandwidth of a window is important. Usually the width of the main lobe of the spectrum of the window is considered, instead of the bandwidth itself. Consequently, a narrow main lobe is desired to minimize the spectral leakage, and accurately reproduce the spectrum. As the main lobe is narrowed, the side lobes increase in amplitude causing spectral leakage and a loss in resolution. Therefore, a trade-off between the main lobe width and side lobe amplitude exists.

A rectangular window has a constant weighting factor of one and merely truncates the sequence. Other windows are weighting functions which taper the sequence to zero or near to zero at each end, trying to minimize the discontinuity at the ends. As the leakage of the estimate of the spectrum is reduced by smoothing the sides of the window, the main lobe is broadened resulting in a loss in resolution between adjacent frequencies.

The number of points of the window, or the window length, does not change the shape of the window spectrum. But the window length affects the width of the main lobe of the window spectrum. As the window length increases, the width of the main lobe decreases. The width of the main lobe is inversely proportional to the window length. Since the length of the data is the same as the window length, lengthening the window increases the number of data points observed. Thus, the effects of truncation are decreased and spectral resolution is increased. Also, the window length (in this case the data length) is directly related to the range resolution. Since each window will produce one profile point, the window length determines the range which corresponds to a profile point. The shorter the window, the smaller the depth increment between profile points.

3.2.2 The Chirp z-Transform Algorithm

Straight lines in the s-plane are mapped into circles or spirals in the z-plane by the relation $z = e^{sT}$. A special case is the imaginary axis. The imaginary axis in the s-plane is mapped into the unit circle in the z-plane. The discrete Fourier transform (DFT) evaluates the z-transform of a sequence at equispaced points along the unit circle. The chirp z-transform algorithm evaluates the z-transform of a sequence at constant angular spaced points along a circular or spiral contour in the z-plane (Rabiner et al., 1969).

The chirp z-transform (CZT) can enhance spectral peaks or resonances, especially if something is known about the location of the poles, because it samples the z-transform over any section of the z-plane. The CZT was used to find the frequency spectrum for this extraction of Doppler information because the approximate location of the poles are known. Furthermore, the CZT can sample the z-transform over a small section of the z-plane. The maximum expected frequency shift from the Doppler signal is much less than 500 kHz. Therefore, the frequency resonances are expected to be found in the area of 4.5-5.5 MHz. It is not necessary to sample the z-transform over the whole z-plane, since the frequencies of interest are in a small range around 5 MHz. Sampling the z-transform over a small section of the z-plane around 5 MHz is desirable.

The z-transform of a finite sequence of N points, computed for a finite number of points z_k is:

$$X_k = X(z_k) = \sum_{n=0}^{N-1} x_n z_k^{-n} \quad . \tag{3-1}$$

If

$$z_k = e^{-j2\pi k/N} \quad , \qquad k = 0,1,\ldots,N-1 \ ,$$

the result is proportional to the DFT. The result is the CZT if

$$z_k = AW^{-k} \quad , \qquad k = 0,1,\ldots,M-1 \ ,$$

where M is an arbitrary number. The two parameters A and W are arbitrary complex numbers of the form:

$$A = A_0 e^{j2\pi\theta_0} \quad , \quad W = W_0 e^{j2\pi\phi_0} \quad .$$

If $A = 1$, $W = e^{-j2\pi/N}$, and $M = N$, then $z_k = e^{-j2\pi k/N}$ and the result reduces to the DFT. The starting point of the contour is $z = A$, and W_0 determines the spiral shape of the contour. If $W_0 = 1$, the contour is a circle. The contour spirals towards the origin in the z-plane as k increases if W_0 is less than one, and spirals outward as k increases if W_0 is greater than one. The angular spacing of the frequency samples is $2\pi\phi_0$.

Summarizing, the CZT is given by:

$$X(z_k) = \sum_{n=0}^{N-1} x_n A^{-n} W^{-nk} \quad . \tag{3-2}$$

The CZT is more flexible than the DFT. The number of z-transform frequency samples, M, does not have to equal N, the number of input data samples. The contour in the z-plane is a circle or spiral and the space of frequency samples is arbitrary. But the DFT, especially if implemented by the fast Fourier transform (FFT), is computed much faster than the CZT because of the large amount of complex multiplications.

Direct computation of the CZT requires NM calculations. By making a substitution this number can be reduced. The expression for the CZT can be rewritten using the identity:

$$nk = 1/2[n^2 + k^2 - (k-n)^2] \quad .$$

The expression becomes:

$$X_k = \sum_{n=0}^{N-1} x_n A^{-n} W^{n^2/2} W^{k^2/2} W^{-(k-n)^2/2} \quad . \tag{3-3}$$

Although the expression appears to be even more complex, it can be viewed as a three step computation. First, the input sequence x_n is multiplied

by $A^{-n}W^{n^2/2}$. Next, the product is convolved with $W^{-n^2/2}$. If $W_0 = 1.0$, then $W^{-n^2/2} = e^{-j\pi n(n\phi_0)}$. This is a linearly increasing frequency sinusoid. Filters of this type are called "chirp" filters, which is where the CZT gets its name. Finally, the result is obtained by multiplying the output of the convolution by $W^{k^2/2}$. The slowest part of the computation is the convolution. A high speed convolution can be performed with the FFT. This reduces the number of computations to approximately $(N+M-1)\log_2(N+M-1)$.

The chirp z-transform algorithm (Figure 3.5) begins with a waveform of N samples, x_n, and the result is M samples of the z-transform, X_k. After the two parameters are chosen, the first step is to define a parameter L, where L is the smallest integer greater than or equal to one less the sum of N and M: $L \geq N+M-1$. Also, L must be compatible for the FFT. Specifically, L must be a power of two. The second step is to compute y_n by multiplying x_n by $A^{-n}W^{n^2/2}$, $n = 0,1,\ldots,N-1$ and zero elsewhere. To implement the convolution, the L point DFT of the product, y_n is taken using the FFT algorithm producing Y_r, $r = 0,1,\ldots,L-1$. Next, v_n is defined:

$$v_n = \begin{cases} W^{-n^2/2} & , \quad 0 \leq n \leq M-1 \\ W^{-(L-n)^2/2} & , \quad L-N+1 \leq n < L \\ \text{arbitrary} & , \quad \text{elsewhere} \end{cases} .$$

If $L = M+N-1$, the arbitrary region of v_n does not exist. To eliminate the arbitrary region, M should be increased. v_n is defined this way to force the results of normal convolution from circular convolution. The L point DFT of v_n is taken using the FFT algorithm producing V_r: $r = 0,1,\ldots,L-1$.

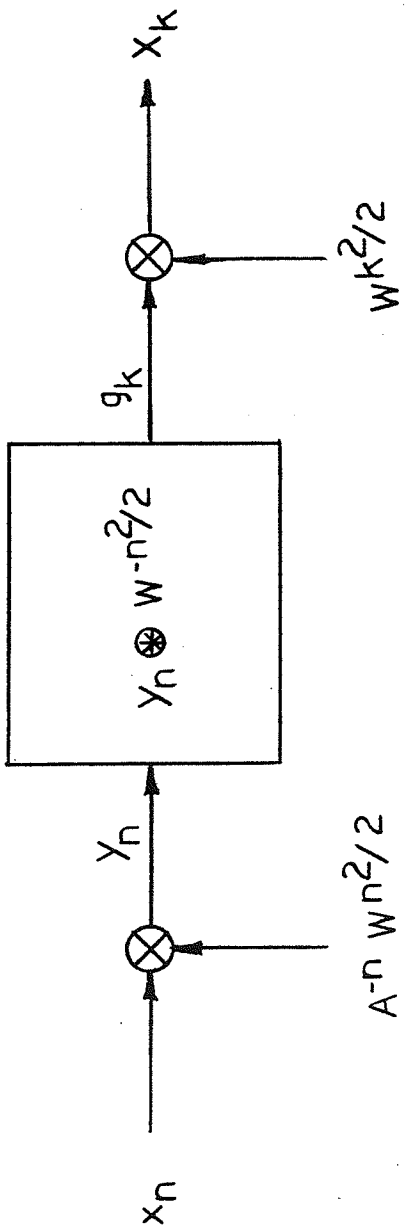

Figure 3.5. The chirp z-transform algorithm.

Next, V_r is multiplied by Y_r, point by point, producing G_r, r = 0,1,...,L-1. To complete the convolution, the L point inverse DFT is taken of G_r, to produce g_k. Finally, the result, X_k, is obtained by multiplying g_k by $W^{k^2/2}$, k = 0,1,...,M-1. The excess points outside this area are discarded.

Two important points to consider when using this algorithm are the space required to store the intermediate filter function, v_n, and the difficulty in calculating $W_0^{n^2/2}$ in some cases. W_0 should be near to 1.0 because it becomes more difficult to compute $W_0^{n^2/2}$ as W_0 decreases. For small W_0 and large n, many digits of accuracy are needed. Ideally, W_0 should be one, since one raised to any power remains one.

3.2.3 Program Description

The program which was used to process the A-scan signals is listed in the Appendix. It was written in Fortran VI, except the FFT subroutine which was written in assembly language to minimize the processing time. The program is user interactive. After dimensioning the arrays and declaring the type of some variables, the program asks for six parameters. They are the number of valid points, the sampling frequency, the center frequency, the bandwidth, the window, and the window length. The number of valid points, NPTS, is the number of data points to be processed. The sampling frequency, FS, is the digitization frequency, 88.45 MHz for all these experiments. The center frequency, CF, and bandwidth, BW, determine the location of the frequency samples in the z-plane. All frequencies should be entered in MHz. The choices of window, WC, are given. Lastly, the window length, WSIZE, must be specified.

After the program reads in the parameters, it reads in the data points, DATA. Before the data points can be processed they must be centered about

zero amplitude, or have zero offset. The program averages out the offset by totaling all the data points, taking the average, and subtracting the average from each point. The zero offset data points are stored in the array FR. Later, they will be replaced by the points of the profile.

Next, the window, WINDOW, is computed according to the window and window length chosen. The arrays are indexed from one to N, the window length, but the window must be computed from zero to N-1. Therefore, one is subtracted from the index in the window equations. The Hamming, Hanning, Blackman, and Blackman-Harris windows all have a common form, and they are grouped together. The triangular window has a different form and it is calculated separately.

After the window is computed, the parameters for the CZT are computed. The CZT is computed on a section of the unit circle. To start on the unit circle, $A_0 = 1.0$. To follow a circular contour, $W_0 = 1.0$. The circle begins at 0 rad/s and continues to 2πFS rad/s. The largest frequency point on the circle is the sampling frequency, or digitization frequency, because only frequency components less than the sampling frequency were captured in digitization. A conversion factor of 2π/FS will be used to locate points on the circle. The location of the starting point on the unit circle is determined by $2\pi\theta_0$, THETA. The frequency samples will extend half the bandwidth on both sides of the center frequency. Therefore, the samples will start at 2π(CF-BW/2)/FS rad/s. PHI, $2\pi\phi_0$, determines the spacing of the frequency samples. The total length of the contour is 2πBW/FS. The number of frequency samples is M. Instead of choosing $L \geq M+N-1$, L was fixed at 1024 and M was determined by M = 1025-N. Therefore, the frequency resolution is determined by the number of data

points to be processed, the length of the window. The number of spaces between the points is one less. Therefore, the length of the contour is divided by the number of spaces to yield the width of the spaces: $2\pi BW/FS(1024-N)$. A center frequency of 5 MHz and a bandwidth of 1 MHz was used for all these experiments, as previously determined.

Before performing the CZT, two other parameters can be computed and stored for later use. The filter function, H, is computed as previously defined in Section 3.2.2, remembering to shift the index down one to start at zero. Also, the first multiplier, T2, can be computed. Remembering A and W are both one and adding the exponents, the result is: $e^{-jn(n\phi/2+\theta)}$.

Next, the main part of the program begins. The window is multiplied by the first data points. Then it is moved over one data point at a time. Each windowed group corresponds to a point of the profile, increasing in depth. At each data point, the following group of data points are windowed and the CZT is used to find the frequency spectrum. The maximum amplitude frequency component of the spectrum is stored as the frequency at that profile point. The number of windowed groups is NPTS - WSIZE + 1. At each data point, the group following it is multiplied by the window function and the first multiplier, point by point. The remaining points, until 1024 points are reached, are set to zero. To convolve the result, X, with the filter function, a 1024 point FFT is taken, point by point. Then they are multiplied together and the inverse FFT is taken.

The second multiplier is not necessary. Since W is one, the multiplier will only effect the phase of the spectrum and not the magnitude. The general shape of the amplitude spectrum increases in amplitude with frequency, reaches a maximum, and decreases in amplitude with frequency.

The single frequency component is smeared due to leakage from truncation. The spectrum was not serrated from the window function as expected and a least squares fit was not necessary. The maximum amplitude frequency for each profile point was found by comparing the amplitude at each spectral point with the next until the amplitude is no longer increasing. The maximum amplitude is at that point. The maximum amplitude spectral point is converted to frequency: $(FS/2)(\text{point} \times \phi + \theta)$. To follow the processing, the points of the profile, the number of the windowed group and its frequency, are displayed at the terminal and stored in the array, FR.

The last third of the program statements is the FFT subroutine. It is written in assembly language to minimize processing time. The parameters which are passed to the subroutine are the points to be processed, the number of those points, and the option parameter. The option is zero for the FFT and one for the inverse FFT.

CHAPTER 4

RESULTS AND DISCUSSION

Different windows were tested to find the one best suited for these data. The necessary characteristics for an appropriate window were found. The velocity profiles for various windows and lengths are discussed. The shape and size of the velocity profiles obtained are compared to the expected results. Finally, the results of varying velocities are examined.

4.1 Window Selection

In order to extract frequency versus depth into the vessel, the digitized A-scan signal for the entire vessel cross section is processed a small block at a time. During processing, each small block of the digitized A-scan signal is multiplied by a window, which enhances the spectral resolution as discussed in Section 3.2.1. The window and its length were determined for the extraction of these Doppler ultrasound data.

The width of the main lobe and the amplitude of the largest sidelobes for ten windows are listed in Table 4.1 (Harris, 1978). The width of the main lobe, listed in bins for comparison, is determined by the 3 dB bandwidth, where each bin is equivalent to $2\pi/N$, and N is the length of the window. The amplitude of the greatest sidelobes for each window is listed in decibels references to the amplitude of the main lobe.

Several sets of data, digitized A-scan signals, were processed with these ten different windows, varying the length of each window, to find the most appropriate window. First, each window was tested with a length of 200 points, and then each was gradually increased to a length of 1000

Table 4.1

Window Characteristics

Window	Main Lobe Width (in bins)*	Sidelobe Amplitude (in dB)**
Rectangular $w(n) = 1.0,\ n = 0,1,\ldots,N-1$	0.89	-13
Triangular (Bartlett) $w(n) = 2n/(N-1),\ n = 0,1,\ldots,(N-1)/2$ $= 2-2n/(N-1),\ n = (N-1)/2,\ldots,N-1$	1.28	-27
Hanning Windows $w(n) = \sin^2(\pi n/(N-1)),\ n = 0,1,\ldots,N-1$		
$a = 1$: $w(n) = \sin(\pi n/(N-1))$	1.20	-23
$a = 2$: $w(n) = \sin^2(\pi n/(N-1))$ $= 0.5-0.5\cos(2\pi n/(N-1))$	1.44	-32
Hamming Window $w(n) = 0.54-0.46\cos(2\pi n/(N-1)),$ $n = 0,1,\ldots,N-1$	1.30	-43
Blackman Window $w(n) = 0.42-0.5\cos(2\pi n/(N-1))$ $+ 0.08\cos(4\pi n/(N-1)),$ $n = 0,1,\ldots,N-1$	1.68	-58
Blackman-Harris Windows $w(n) = a_0-a_1\cos(2\pi n/(N-1))+a_2\cos(4\pi n/(N-1))$ $-a_3\cos(6\pi n/(N-1)),$ $n = 0,1,\ldots,N-1$		
a_0 a_1 a_2 a_3		
0.42323 0.49755 0.07922 --	1.66	-67
0.44959 0.49364 0.05677 --	1.56	-61
0.35875 0.48829 0.14128 0.01168	1.90	-92
0.40217 0.49703 0.09392 0.00183	1.74	-44

N is the length of the window.

*Main lobe width, in bins, is the 3 dB bandwidth, where bin = $2\pi/N$.

**Sidelobe amplitude is the largest sidelobe level reference to the main lobe.

points. When processing the data, not just one window produced the expected parabola. Each window reached a length at which the result was parabolic. Also, increasing the length of the window beyond its threshold length worked. The corresponding characteristics, such as main lobe width, were compared for each window at its threshold length.

It was observed that the maximum main lobe width which could follow the frequency spectrum due to fluid flow was 0.0136 rad/sec. This corresponds to a Hamming window of length 600, a triangular window of length 592, and a Hanning window of length 665, for example. A larger main lobe could not follow the flow spectrum across the whole profile as shown with trial 21c processed with a length 500 Hamming window (Figure 4.1). The expected velocity profile and corresponding frequency spectrum should be parabolic. Increasing the length of the window to 600 points, or decreasing the main lobe width to 0.0136 rad/sec, produces the expected parabolic curve (Figure 4.2). Increasing the length of the window beyond the necessary 600 points to 700 points (Figure 4.3) not only decreases the length of the profile curve by losing half the number of points decreased at each end as expected, but smoothes and flattens the spectrum as well. Increasing the window length to 600 points, increases the spectral resolution by narrowing of the main lobe. With the window length increased beyond 600 points, the main lobe is too narrow to view the whole data spectrum.

Also, the different windows have different smoothing effects on the spectrum, as expected. Each window has different amplitudes of the maximum sidelobe and different rates in which the sidelobes decrease. Trial 21c was processed with several windows, each one with approximately

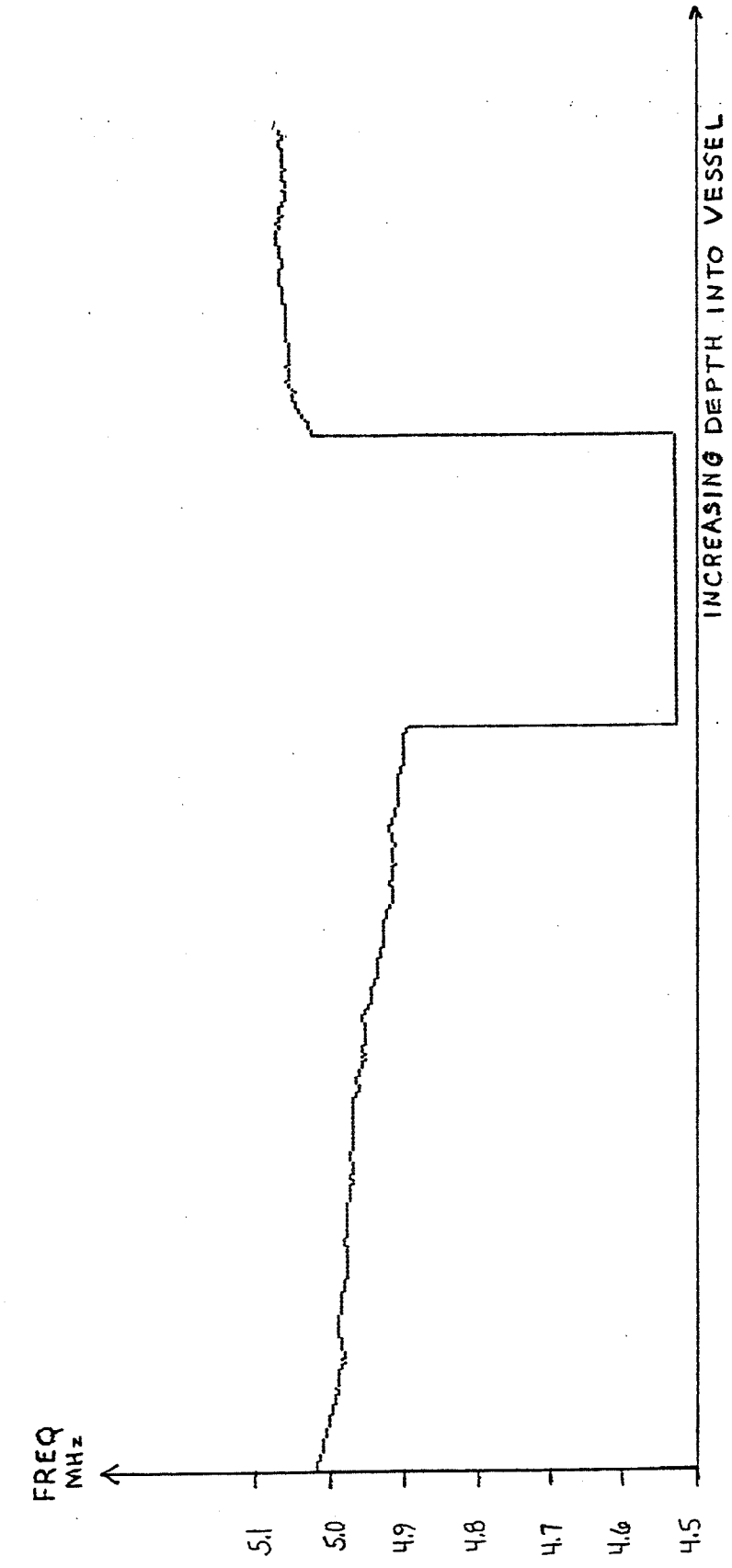

Figure 4.1. Trial 21c (approximate flow rate: 1.8 m/s, away from the transducer) processed with a Hamming window, length 500.

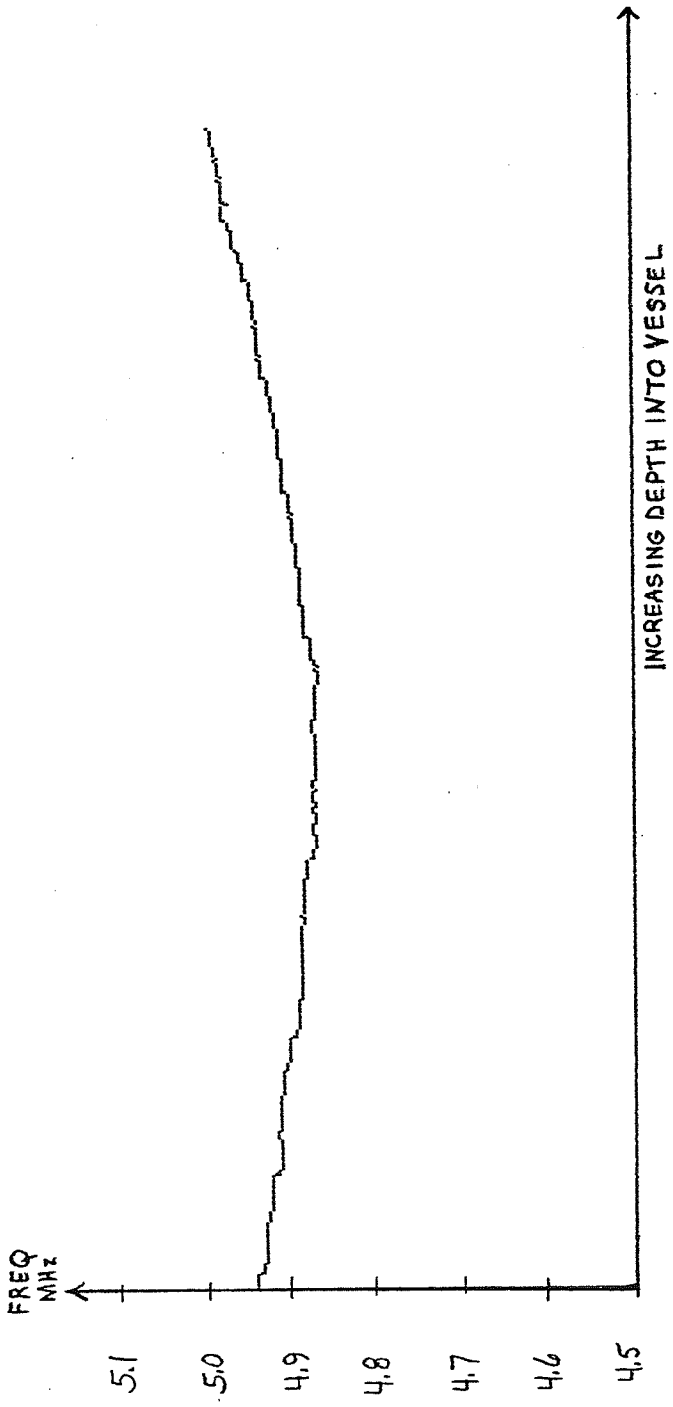

Figure 4.2. Trial 21c processed with a Hamming window, length 600.

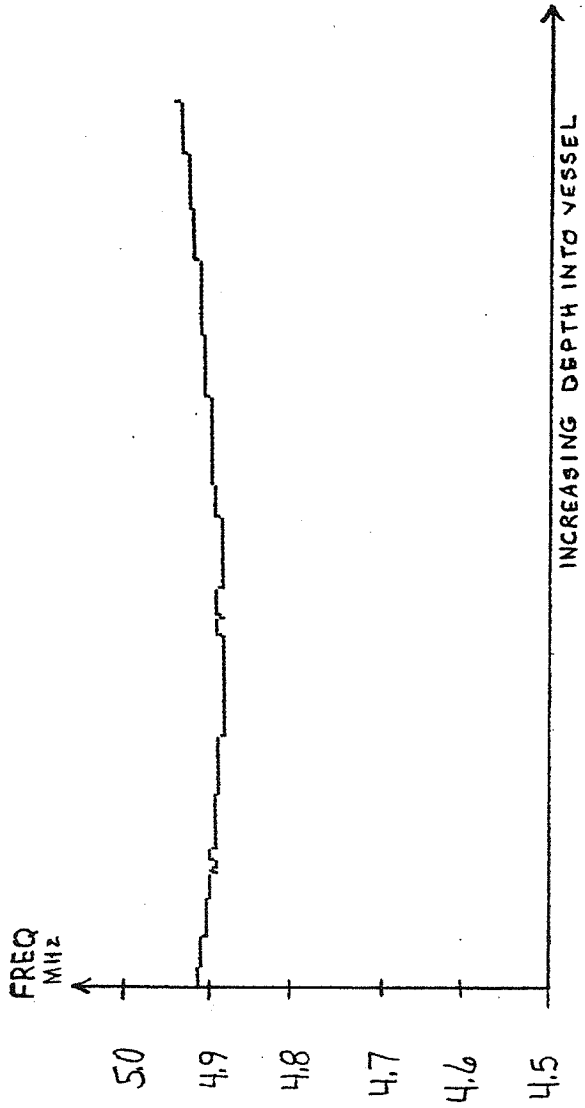

Figure 4.3. Trial 21c processed with a Hamming window, length 700.

the same main lobe width. The curves are shown in Figure 4.2 and Figures 4.4-4.7. The Hanning window (Figure 4.2) produces the roundest parabola. The triangular window (Figure 4.4) smoothes the profile somewhat. The Blackman window (Figure 4.6) and the Blackman-Harris windows, as represented by a 4-term, -92 dB sidelobe amplitude, Blackman-Harris window (Figure 4.7) smooth and flatten the profile too much to tell the true maximum frequency shift and where it occurs. Therefore, a Hamming window or triangular window was chosen to process further data because of the high spectral resolution.

Another reason for choosing the Hamming window or triangular window to process the data was their threshold window length. Of the ten windows that were tested, the Hamming window and triangular window were the shortest windows that could be used and therefore, they required the smallest number of data points to produce a point of the profile. Both windows required 600 data points to produce one profile point, corresponding to an axial depth in tissue of about 5.0 mm, which is less than one-third of the vessel diameter. Consequently, less than one-third of the vessel information was used at a time. Also, using fewer data points to produce one profile point, more profile points could be obtained from the received signal. Furthermore, the technique could be used on smaller vessel.

The spectral resolution depends on the length of the window. The frequency samples are equally spaced along the chosen path in the z-plane. The resolution can be determined by dividing the bandwidth by the number of frequency samples: 1024 - (window length). Therefore, another reason for choosing the shortest window, Hamming window or triangular window of

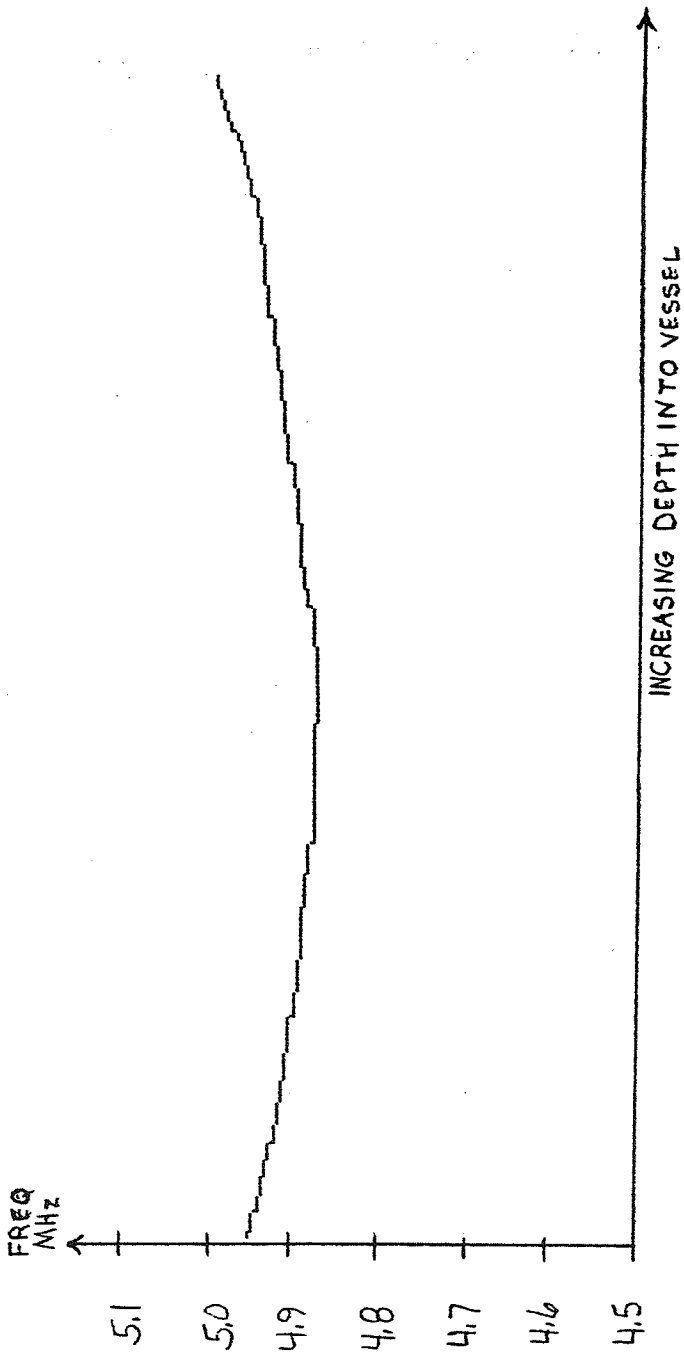

Figure 4.4. Trial 21c processed with a triangular window, length 600.

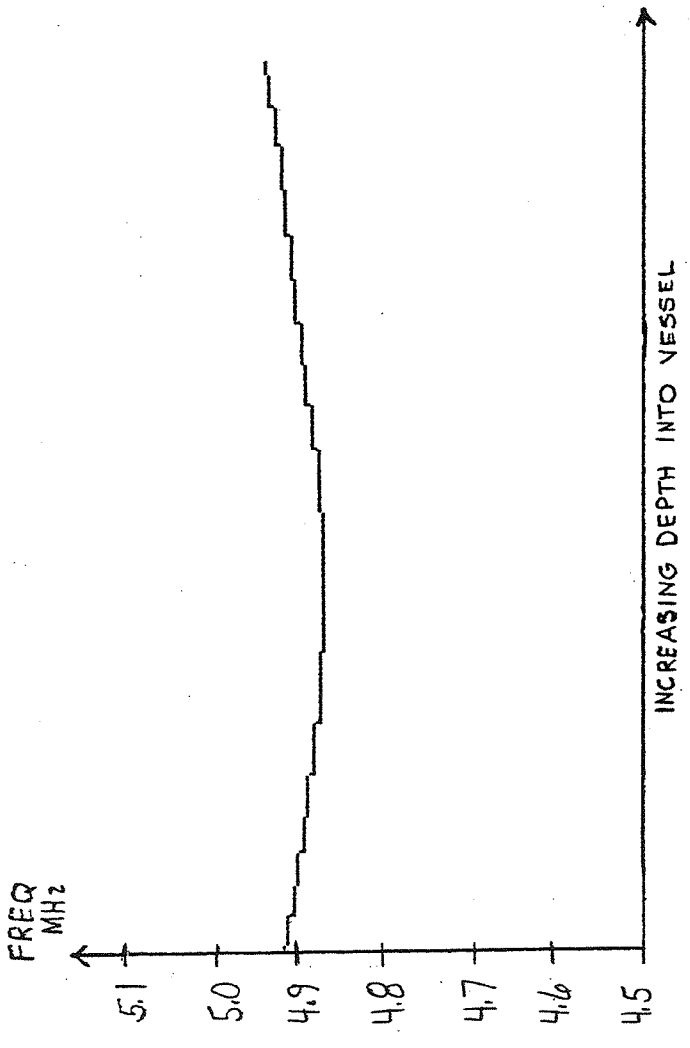

Figure 4.5. Trial 21c processed with a Hanning window, length 700.

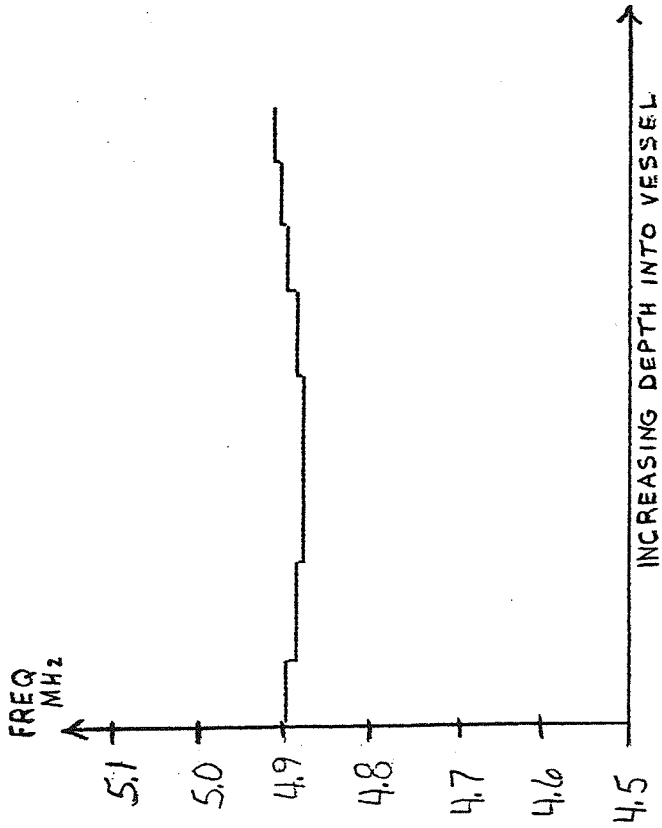

Figure 4.6. Trial 21c processed with a Blackman window, length 800.

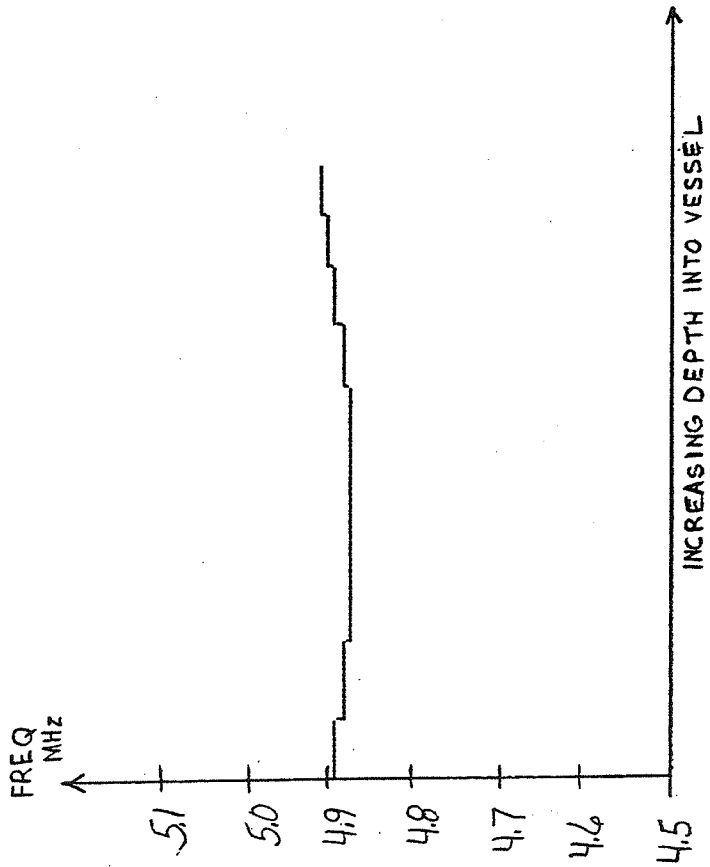

Figure 4.7. Trial 21c processed with a 4-term, -92 dB sidelobe, Blackman-Harris window, length 800.

length 600, is because a shorter window will produce better resolution. For a 1 MHz bandwidth and a window length of 600, the resolution is 2.4 kHz. Experimentally, the resolution was 4.3 kHz.

4.2 Velocity Profiles

The shape of the velocity profiles were parabolic as expected. But, the length of the profiles were slightly shorter than expected. For example, the profile of trial 21b (Figure 4.8) is 1050 points or 8.8 mm. long, as compared to the vessel diameter of 15.9 mm. This could be caused by the ultrasound beam not being centered, but slightly above the middle of the vessel, and because the beginning and the end of the Doppler signal is overwhelmed by the large reflected signal from the vessel walls.

The effects of varying the velocity can be seen in Figures 4.8-4.11. As the velocity increases, the parabola becomes larger with a corresponding greater maximum frequency shift. Also, as the velocity increases, the length of the profile lengthens, possibly because the main lobe could follow the signal, or because the Doppler signal is not as overwhelmed by the echo from the vessel walls. For zero velocity conditions (Figure 4.9), the profile is not flat, but gradually decreases across the vessel. This can be explained by the constantly increasing attenuation as a function of frequency with distance, and by the oblique angle at which the ultrasound beam is transmitted. Therefore, the correct velocity profile is obtained by subtracting the profile of a signal due to zero velocity from the profile of a signal under the same conditions except a change in velocity. Some of this error could be corrected by knowing the exact angle the beam subtends with the vessel and the frequency dependence of attenuation, so

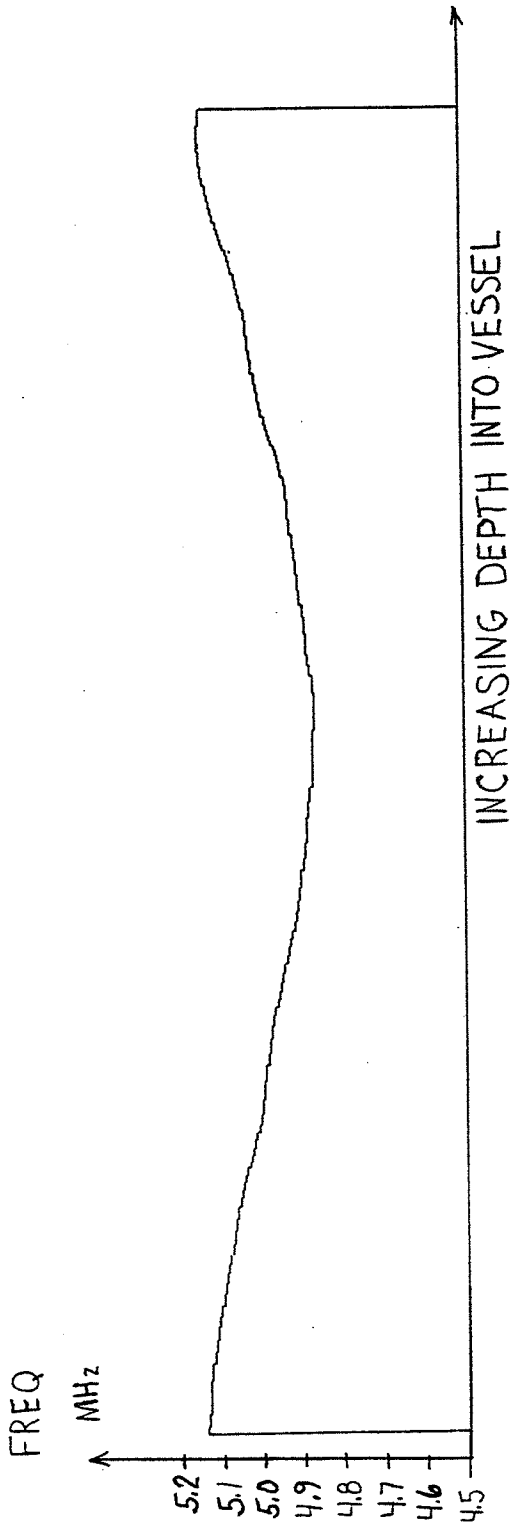

Figure 4.8. Trial 21b (approximate flow rate: 1.8 m/s, away from the transducer) processed with a triangular window, length 600.

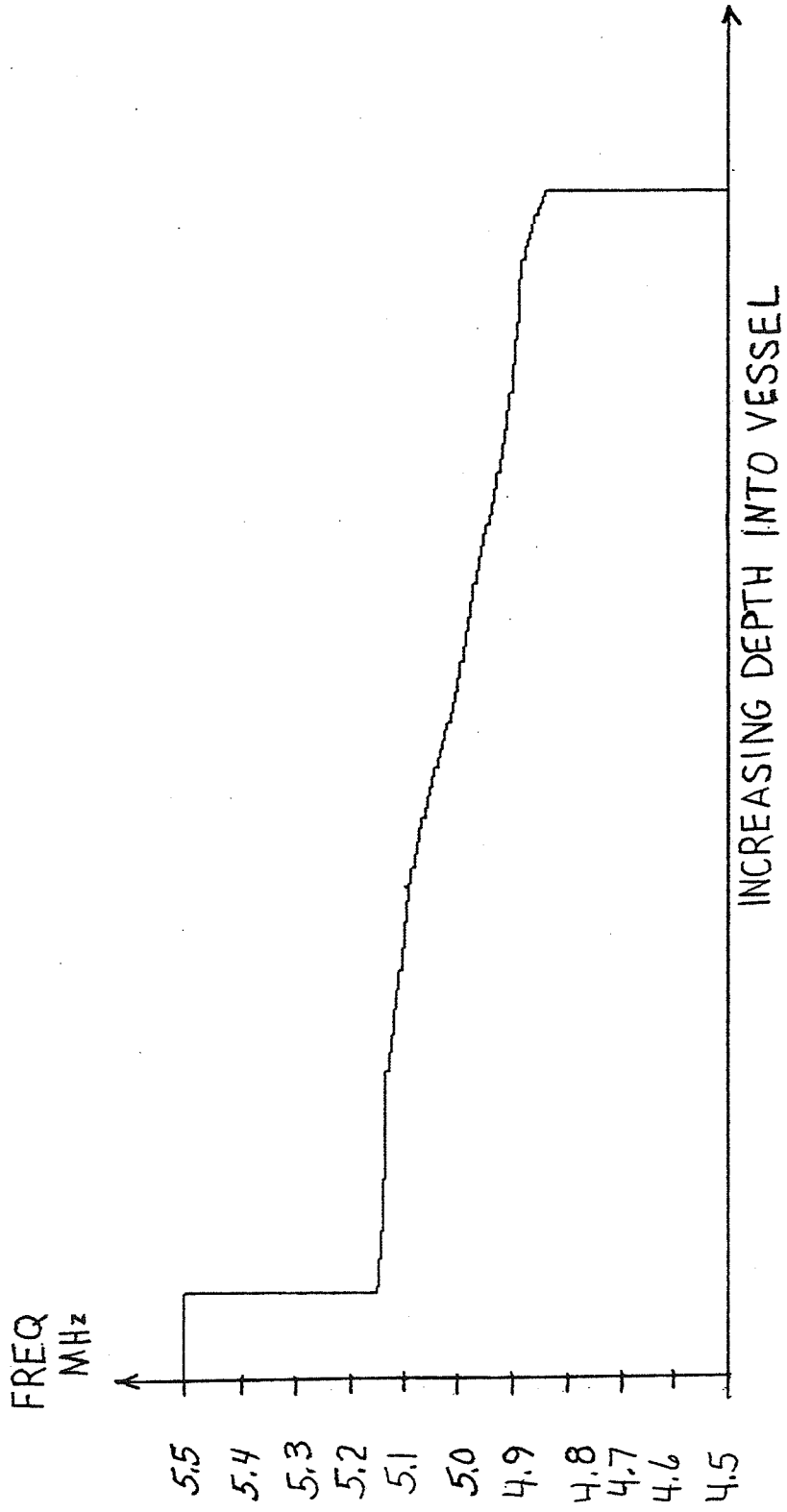

Figure 4.9. Trial 23 (approximate flow rate: 0 m/s) processed with a triangular window, length 600.

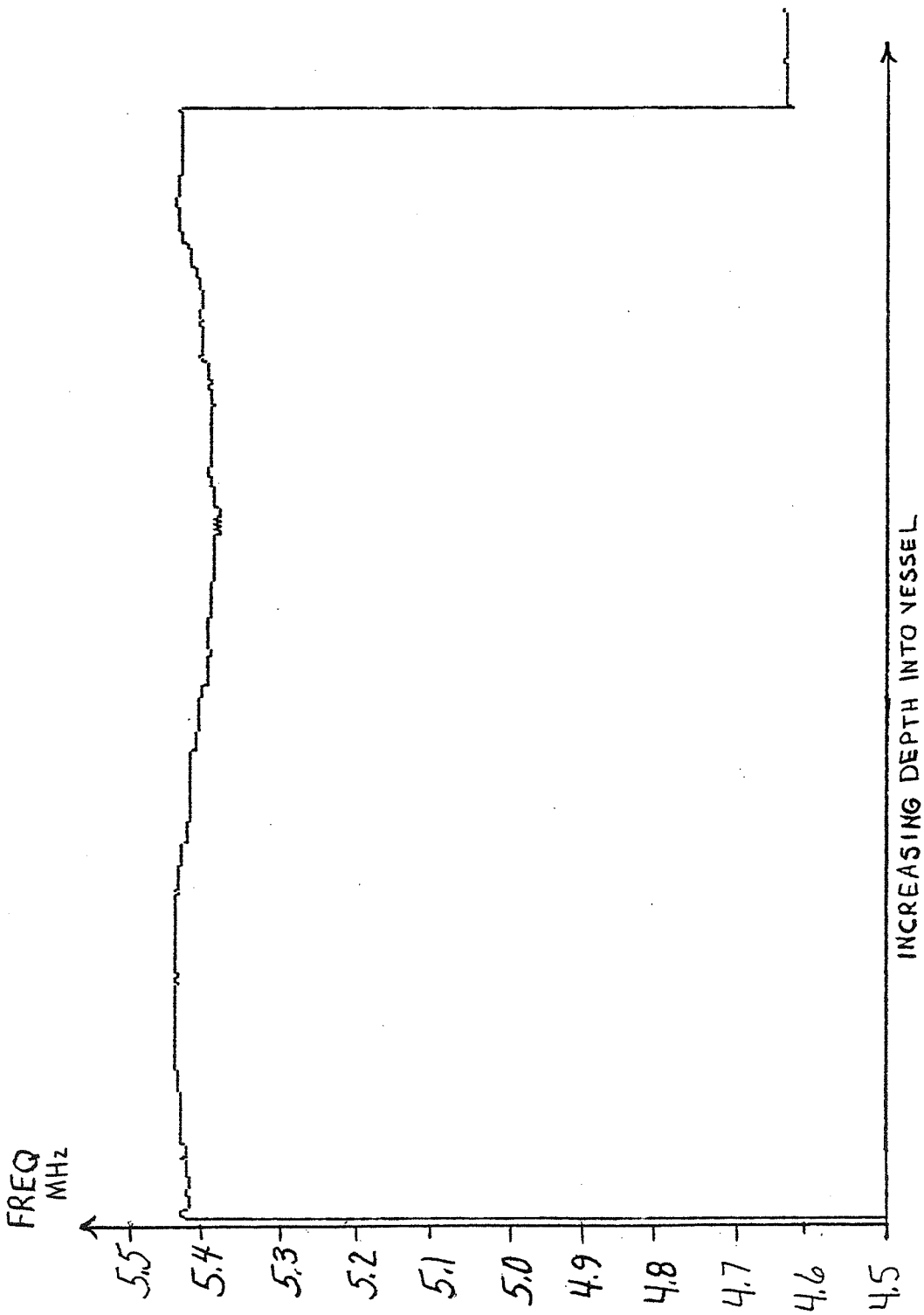

Figure 4.10. Trial 28 (approximate flow rate: 2 m/s, away from the transducer) processed with a triangular window, length 650.

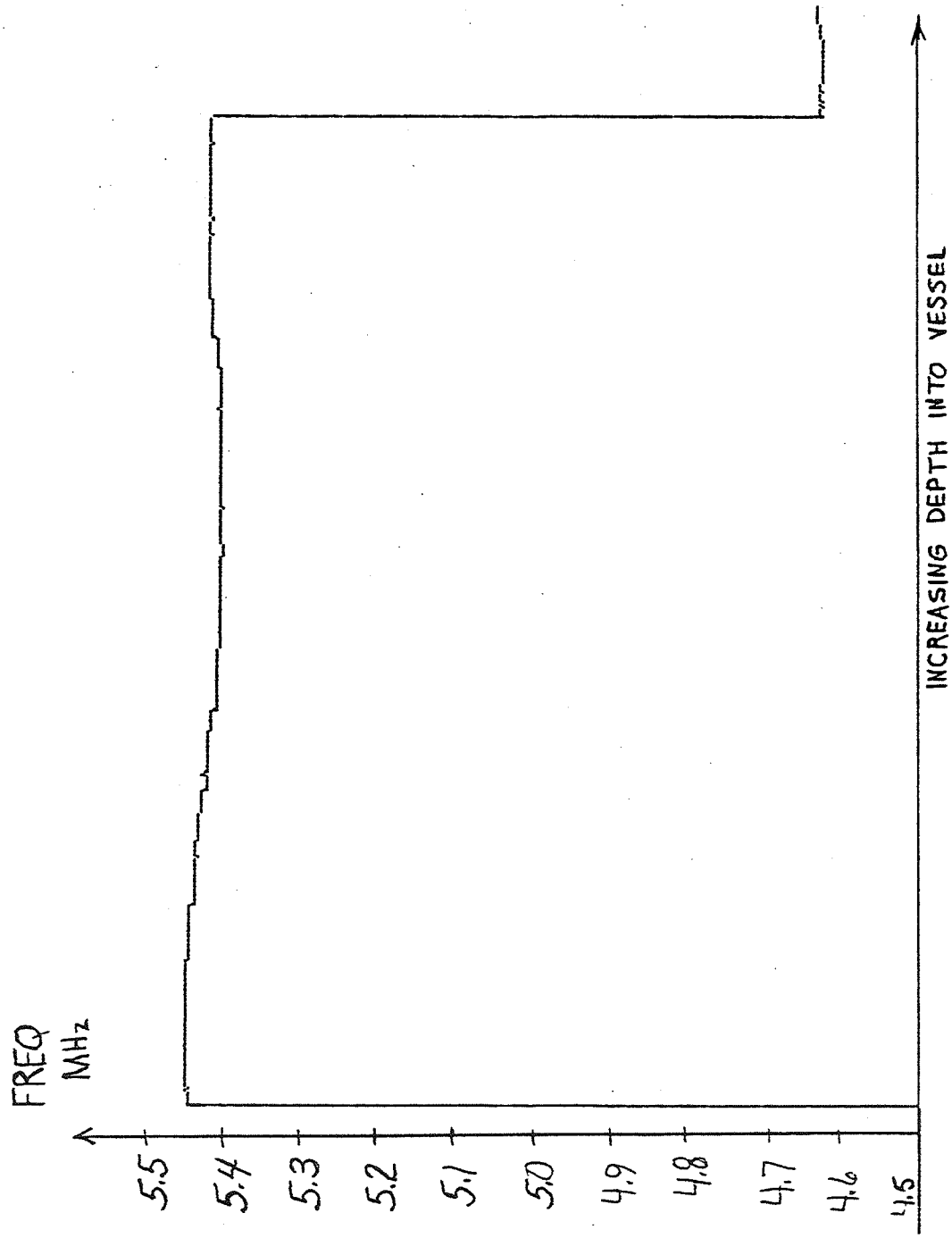

Figure 4.11. Trial 32 (approximate flow rate: 0.3 m/s, away from the transducer) processed with a triangular window, length 650.

that a time gain compensation function could be multiplied to each data window to account for the increasing attenuation.

CHAPTER 5

PROBLEMS AND IMPROVEMENTS

Several problems encountered in these experiments using this chirp z-transform processing technique were not resolved. One of the problems encountered is the magnitudes of the frequencies of the parabolic profiles which are different than expected. The frequency at the stationary vessel walls is not constant from trial to trial and varies depending on the exact position of the transducer. If the transducer is not changed and the velocity of the fluid is changed, the frequency shift at the stationary vessel walls is the same. For example, trial 21b (Figure 4.8) and trial 23 (Figure 4.9) were both taken without moving the transducer, but changing the velocity. The frequency at the first wall from the profiles of both trials is 5.14 MHz while that of the next set (Figures 4.10-4.11) is 5.45 MHz. Therefore, the frequency shift used to determine the velocity of the fluid was calculated each time by comparing the frequency of the walls to that of the points of the parabola.

Another problem encountered is the magnitude of the frequency shift and corresponding velocity of the fluid which is greater than expected. The maximum change in frequency is 273.6 kHz for trial 21 which corresponds to a maximum velocity of 60 m/s. The expected maximum velocity was 10 m/s, or less. The initial flow measurements were not accurate, however. The technique, as described in Section 2.2.2, is subject to large errors and was only done initially, to calculate the order of magnitude of the velocities and frequency shifts expected.

Therefore, in order to quantify the fluid velocity, several improvements could be made, after the flow is measured accurately. Knowledge of

the exact angle between the transducer and the vessel, and the frequency dependence of attenuation is important to quantify the fluid velocity, as mentioned in Section 4.2. Therefore, an improvement to this technique could be an accurate measurement of the angle between the transducer and the vessel. Initially, this could be implemented by a mechanical positioning device to hold the transducer. This angle measurement technique would be suitable for these experiments, but it is invasive. Eventually, the angle measurement could be determined non-invasively from an ultrasonic image obtained simultaneously with the Doppler signal, showing the vessel and the path of the sound beam used for the Doppler measurement.

In addition to obtaining the angle, the distance from the transducer to the vessel could be obtained from either method. This distance would be useful in implementing a time gain compensation function which would be multiplied to the data before processing to account for the increasing attenuation of the ultrasonic wave with distance. Also, the function depends on the intervening medium and frequency. Measurements would be made on the system, using several different intervening media besides water, to accurately determine the function.

The results could possibly be improved by shaping the transmitted ultrasonic wave. The current experiment uses a relatively short pulse. Shaping of the transmitted pulse will effect the output, since it changes the frequency spectrum of the transmitted wave. Varying the shape and length of the transmitted pulse could improve the transmitted spectrum and therefore, the resulting velocity profiles.

In conclusion, these experiments demonstrated that this digital processing technique for Doppler ultrasound flowmetery signals, in principal, is feasible. The velocity profiles obtained from a tube of flowing milk were parabolic, suggestive of simple laminar flow. Although the magnitude of the fluid velocities were not correct, the velocity profiles were of the proper shape. Optimization of various parameters, as discussed, should yield a quantitatively accurate velocity profile.

REFERENCES

Baker, D. W., F. K. Forster, and R. E. Daigle. Doppler Principles and Techniques in Ultrasound: Its Applications in Medicine and Biology, F. J. Fry, ed. New York: Elsevier Scientific Publishing Company, 1978.

Barber, F. E., D. W. Baker, A. W. Nation, D. E. Strandness, Jr., and J. M. Reid. "Ultrasonic Duplex Echo Doppler Scanner," IEEE Trans. Biomed. Eng., BME-21(2), 1974, 109-133.

Bergel, D. W., ed. Cardiovascular Fluid Dynamics, 2 vols. New York: Academic Press, Inc., 1972.

Childers, D. and A. Durling. Digital Filtering and Signal Processing. New York: West Publishing Company, 1975.

Choi, W. K. "Spectral Analysis of Doppler Ultrasonic Flowmeter Signals." M.S. Thesis, Department of Electrical Engineering, University of Illinois, Urbana, Illinois, 1978.

Cox, R. H. "Comparison of Linearized Wave Propagation Models for Arterial Blood Flow Analysis," J. Biomechanics, 2(3), July 1969, 251-265.

Flax, S. W., J. G. Webster, and S. J. Updike. "Statistical Evaluation of the Doppler Ultrasonic Blood Flowmeter," ISA Trans., 10(1), 1971, 1-20.

Foster, S. G. "An Image Digitizing System for a Scanning Laser Acoustic Microscope." M.S. Thesis, Department of Electrical Engineering, University of Illinois, Urbana, Illinois, 1981.

Goss, S. A., R. L. Johnston, and F. Dunn. "Comprehensive Compilation of Empirical Ultrasonic Properties of Mammalian Tissues," J. Acoust. Soc. Am., 64(2), August 1978, 423-457.

Harris, F. J. "On the Use of Windows for Harmonic Analysis with the Discrete Fourier Transform," Proc. IEEE, 66(1), January 1978, 51-83.

Kufahl, R. H. "Numerical Solution of Unsteady Viscous Flow in Looping Arterial Networks." Ph.D. Thesis, Department of Mechnical Engineering, University of Illinois, Urbana, Illinois, 1980.

Noordergraf, A. Hemodynamics in Biological Engineering, H. P. Schwann, ed. New York: McGraw Hill, 1969.

Noordergraf, A., ed. Circulatory System Dynamics. New York: Academic Press, Inc., 1978.

Pao, R. H. F. Fluid Mechanics. New York: John Wiley and Sons, Inc., 1961.

Rabiner, L. R., R. W. Schafer, and C. M. Rader. "The Chirp z-Transform Algorithm and Its Application," Bell System Technical Journal, 48, May-June 1969, 1249-1292.

Roberson, J. A. and C. T. Crowe. Engineering Fluid Mechanics. Boston: Houghton Mifflin Company, 1975.

Sharpe, G. J. Fluid Analysis. New York: American Elsevier Publishing Company, Inc., 1967.

Shung, K. K., R. A. Sigelmann, and J. M. Reid. "Scattering of Ultrasound by Blood," IEEE Trans. Biomed. Eng., BME-23(6), November 1976, 460-467.

Wintrobe, M. M. Clinical Hematology, 6th Ed. Philadelphia: Lea and Febiger, 1967.

APPENDIX: THE PROGRAM

This Appendix is a listing of the program used to process the A-scan signals. A description of the program is given in Section 3.2.3. The main portion of the program is written in Fortran VI and the fast Fourier transform (FFT) subroutine is written in assembly language. The lines beginning with '$', such as the first and last lines, are control cards needed to run the program on the Perkin-Elmer 7/32 computer. In the Fortran language, lines beginning with 'C' are comment statements.

```
1       $BATCH
2       C ***********************************************************
3       C *  A PROGRAM FOR PROCESSING DOPPLER ULTRASOUND DATA  *
4       C ***********************************************************
5             COMPLEX X(1024),H(1024),T2(1023)
6             INTEGER*4 DATA(2048),WSIZE,WC
7             REAL FR(2048),WINDOW(1023)
8       C ***********      ENTER   PARAMETERS          ***********
9             WRITE(1,1)
10          1   FORMAT('ENTER NUMBER OF VALID POINTS (I4)')
11            READ(1,2)NPTS
12          2   FORMAT(I4)
13            WRITE(1,3)
14          3   FORMAT('ENTER SAMPLING FREQ, IN MHZ(F7.2)')
15            READ(1,4)FS
16          4   FORMAT(F7.2)
17            WRITE(1,6)
18          6   FORMAT('ENTER CENTER FREQ AND BANDWIDTH, IN MHZ')
19            READ(1,7)CF,BW
20          7   FORMAT(F10.5)
21            WRITE(1,8)
22          8   FORMAT('ENTER WINDOW SIZE(I3)')
23            READ(1,9)WSIZE
24          9   FORMAT(I3)
25            WRITE(1,11)
26          11  FORMAT('ENTER WINDOW CHOICE:')
27            WRITE(1,12)
28          12  FORMAT('1-RECTANGULAR  6-BLACKMAN')
29            WRITE(1,14)
30          14  FORMAT('2-TRIANGULAR   7-BLACK  -3TERM,-67')
31            WRITE(1,16)
32          16  FORMAT('3-HAMMING      8- MAN   -3    ,-61')
33            WRITE(1,17)
34          17  FORMAT('4-HANNING,SIN2 9-HARRIS -4TERM,-92')
35            WRITE(1,18)
36          18  FORMAT('5-HANNING,SIN 10-     -4    ;-44')
37            READ(1,13)WC
38          13  FORMAT(I1)
39      C *******    READ DATA AND AVERAGE OUT OFFSET    *******
40            SUM1=0.0
41            DO 10 I=1,NPTS
42            READ(2,19)DATA(I)
43          19  FORMAT(I8)
44            SUM1=SUM1+DATA(I)
45          10  CONTINUE
46            SUM1=SUM1/NPTS
47            DO 15 I=1,NPTS
48            FR(I)=DATA(I)-SUM1
49          15  CONTINUE
50      C ***********      CALCULATE  WINDOW          **********
51            DO 40 I=1,WSIZE
52            T1=6.28318*FLOAT(I-1)/FLOAT(WSIZE-1)
53            GO TO(41,40,42,43,44,45,46,47,48,49),WC
54          41  WINDOW(I)=1.0
55            GO TO 40
56          42  WINDOW(I)=0.54-0.46*COS(T1)
```

```
57            GO TO 40
58         43 WINDOW(I)=0.5-0.5*COS(T1)
59            GO TO 40
60         44 WINDOW(I)=SIN(T1/2.0)
61            GO TO 40
62         45 WINDOW(I)=0.42-0.5*COS(T1)+0.08*COS(2.0*T1)
63            GO TO 40
64         46 WINDOW(I)=0.42323-0.49755*COS(T1)+0.07922*
65           1COS(2.0*T1)
66            GO TO 40
67         47 WINDOW(I)=0.44959-0.49364*COS(T1)+0.05677*
68           1COS(2.0*T1)
69            GO TO 40
70         48 WINDOW(I)=0.35875-0.48829*COS(T1)+0.14128*
71           1COS(2.0*T1)-0.01168*COS(3.0*T1)
72            GO TO 40
73         49 WINDOW(I)=0.40217-0.49703*COS(T1)+0.09392*
74           1COS(2.0*T1)-0.00183*COS(3.0*T1)
75         40 CONTINUE
76            IF(WC.NE.2)GO TO 60
77            WC=WSIZE/2-1
78            DO 50 I=1,WC
79            WINDOW(I)=2.0*FLOAT(I-1)/FLOAT(WSIZE-1)
80         50 CONTINUE
81            WC=WC+1
82            DO 55 I=WC,WSIZE
83            WINDOW(I)=2.0-2.0*FLOAT(I-1)/FLOAT(WSIZE-1)
84         55 CONTINUE
85            WC=2
86         60 CONTINUE
87       C *** CALCULATE THETA, PHI, MULTIPLICATIVE FACTOR ***
88       C ********** AND FILTER FUNCTION **********
89            THETA=(CF-BW/2.0)/FS*6.28318
90            PHI=BW/FS*6.28318/(1024-WSIZE)
91            I2=1024-WSIZE+1
92            DO 70 I=1,I2
93            T1=FLOAT(I-1)
94            H(I)=CEXP(CMPLX(0.0,PHI*T1*T1/2.0))
95         70 CONTINUE
96            I2=I2+1
97            DO 75 I=I2,1024
98            T1=FLOAT(1025-I)
99            H(I)=CEXP(CMPLX(0.0,PHI*T1*T1/2.0))
100        75 CONTINUE
101           CALL FFT(H,10,0)
102           DO 80 I=1,WSIZE
103           T1=FLOAT(I-1)
104           T2(I)=CEXP(CMPLX(0.0,-T1*(T1*PHI/2.0+THETA)))
105        80 CONTINUE
106      C ***** RUNNING SPECTRAL ESTIMATION USING CZT *****
107           KOUNT=NPTS-WSIZE+1
108           DO 200 K=1,KOUNT
109           DO 90 I=1,WSIZE
110           J=I+K-1
111           X(I)=T2(I)*FR(J)*WINDOW(I)
112        90 CONTINUE
```

```
      I1=WSIZE+1
      DO 95 I=I1,1024
      X(I)=(0.0,0.0)
   95 CONTINUE
      CALL FFT(X,10,0)
      DO 100 I=1,1024
      X(I)=X(I)*H(I)
  100 CONTINUE
      CALL FFT(X,10,1)
C ***   FIND MAXIMUM AMPLITUDE FREQUENCY COMPONENT   ***
C ************        AT  EACH  DEPTH         ************
      AMAX=0.0
      IMAX=0
      DO 110 I=1,I2
      IF(AMAX.GE.CABS(X(I))) GO TO 110
      AMAX=CABS(X(I))
      IMAX=I-1
  110 CONTINUE
      FREQ=FS(THETA+IMAX*PHI)/6.28318
      WRITE(1,111)K,FREQ
  111 FORMAT(I4,5X,F16.8)
      WRITE(3,131)FREQ
  131 FORMAT(F16.8)
      FR(K)=FREQ
  200 CONTINUE
      STOP
      END
C *****     FAST FOURIER TRANSFORM  SUBROUTINE      *****
C ***********       OPT=0  FOR DFT                ***********
C ***********       OPT=1  FOR INVERSE DFT        ***********
      SUBROUTINE FFT(A,M,OPT)
      COMPLEX A(1),U,W,T
      INTEGER*4 S1(16),S2(16),S,OPT
      N=2**M
$ASSM
          STM   0,S1
          LIS   1,8
          LR    2,1
          L     3,N
          SIS   3,2
          SLLS  3,3
          L     4,N
          SLLS  4,2
          LIS   5,0
          L     10,A
LOOP3     LR    6,4
LOOP4     CLR   5,6
          BTFS  8,JUMP1
          SR    5,6
          SRLS  6,1
          B     LOOP4
JUMP1     AR    5,6
          CLR   1,5
          BFC   8,JUMP2
          L     6,0(1,10)
          L     7,4(1,10)
```

```
169                 L       8,0(5,10)
170                 L       9,4(5,10)
171                 ST      6,0(5,10)
172                 ST      7,4(5,10)
173                 ST      8,0(1,10)
174                 ST      9,4(1,10)
175       JUMP2     BXLE    1,LOOP3
176                 LM      0,S1
177       $FORT
178             PI=3.1415926535
179             S=-1
180             IF(OPT.EQ.1)S=1
181             DO 20 L=1,M
182             LE=2**L
183             LE1=LE/2
184             U=(1.0,0.0)
185             W=CMPLX(COS(PI/LE1),S*SIN(PI/LE1))
186       $ASSM
187                 STM     0,S1
188                 STME    0,S2
189                 LE      0,U
190                 LE      2,U+4
191                 LIS     0,0
192                 LIS     1,8
193                 L       2,LE1
194                 SIS     2,1
195                 SLLS    2,3
196                 L       6,LE1
197                 SLLS    6,3
198       LOOP1     L       3,A
199                 AR      3,0
200                 L       4,LE
201                 SLLS    4,3
202                 L       5,N
203                 SIS     5,1
204                 SLLS    5,3
205                 AR      5,3
206       LOOP2     LE      4,0(3,6)
207                 LE      6,4(3,6)
208                 LER     8,4
209                 LER     10,6
210                 MER     4,0
211                 MER     6,2
212                 MER     8,2
213                 MER     10,0
214                 SER     4,6
215                 AER     10,8
216                 LE      6,0(3)
217                 LE      8,4(3)
218                 LER     12,6
219                 LER     14,8
220                 AER     12,4
221                 AER     14,10
222                 SER     6,4
223                 SER     8,10
224                 STE     6,0(3,6)
```

```
225                 STE   8,4(3,6)
226                 STE   12,0(3)
227                 STE   14,4(3)
228                 BXLE  3,LOOP2
229                 LE    4,W
230                 LE    6,W+4
231                 LER   8,6
232                 LER   10,6
233                 MER   8,2
234                 MER   10,0
235                 MER   0,4
236                 MER   2,4
237                 SER   0,8
238                 AER   2,10
239                 BXLE  0,LOOP1
240                 LME   0,S2
241                 LM    0,S1
242       $FORT
243         20    CONTINUE
244               IF(OPT.EQ.0) GO TO 100
245       $ASSM
246                 STM   0,S1
247                 STME  0,S2
248                 L     1,A
249                 LIS   2,8
250                 L     3,N
251                 SIS   3,1
252                 SLLS  3,3
253                 AR    3,1
254                 L     4,N
255                 FLR   0,4
256       LOOP5     LE    2,0(1)
257                 LE    4,4(1)
258                 DER   2,0
259                 DER   4,0
260                 STE   2,0(1)
261                 STE   4,4(1)
262                 BXLE  1,LOOP5
263                 LME   0,S2
264                 LM    0,S1
265       $FORT
266          100  CONTINUE
267               RETURN
268               END
269       $BEND
```